

# Roll-to-Roll Advanced Materials Manufacturing DOE Laboratory Consortium - FY 2016 Final Report

ORNL/TM-2016/695

December 2016

Funding provided by:

U.S. Department of Energy  
Office of Energy Efficiency and Renewable Energy  
Advance Manufacturing Office



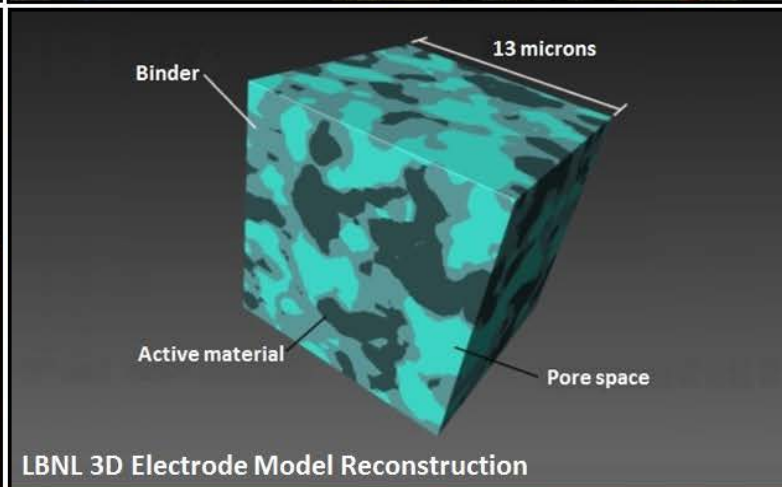
ORNL Dual Slot Die Coater



ANL Advanced Electrode Coater



NREL Small-scale Manufacturing Webline



LBNL 3D Electrode Model Reconstruction



## Disclaimer

This report was prepared as an account of work sponsored by an agency of the United States government. Neither the United States government nor any agency thereof, nor any of their employees, makes any warranty, express or implied, or assumes any legal liability or responsibility for the accuracy, completeness, or usefulness of any information, apparatus, product, or process disclosed or represents that its use would not infringe privately owned rights. Reference herein to any specific commercial product, process, or service by trade name, trademark, manufacturer, or otherwise does not necessarily constitute or imply its endorsement, recommendation, or favoring by the United States government or any agency thereof. The views and opinions of authors expressed herein do not necessarily state or reflect those of the United States government or any agency thereof.

## Foreword

Oak Ridge National Laboratory (ORNL), Argonne National Laboratory (ANL), Lawrence Berkeley National Laboratory (LBNL), and the National Renewable Energy Laboratory (NREL) in collaboration with Eastman Kodak Business Park (Kodak) and Citrine Informatics (Citrine) formed a consortium to broadly disseminate materials, process science, and advanced technologies to industry in the area of R2R manufacturing. This multi-laboratory and industry partnership will enable advanced R2R manufacturing research and development to demonstrate a new materials genomic approach to optimization of process parameters for finding new transformational improvements in manufacturing technologies enabling “green” energy applications. During a one year four lab consortium seed effort, the labs have successfully demonstrated their combined capabilities for a fast clean energy manufacturing development in Fiscal Year (FY) 2016. The first topic for demonstration was on Li-ion battery manufacturing. This consortium creates a national critical team of experts covering all needed aspects from materials genome modeling and simulation through powder materials synthesis, slurry formulation and scale-up, pilot deposition and curing process development, non-destructive process evaluation, big data analytics and validation, to full scale production of rolled goods. This new approach will enable an order of magnitude shorter process development cycles bringing it from 20 years down to two years with the pathway for initial commercialization within months of that.

DOE cost targets for advanced energy storage and conversion applications will not be met without significant and timely advancements in R2R manufacturing. Required R2R advances include adaptation of existing processing methods and development of novel methods that have the potential to significantly impact U.S. manufacturing sector recovery, environmental security, energy security, and sustainable transportation adoption. *Economies of scale through increased manufacturing volumes based on traditional assembly and processing methods will not suffice.* For example, current baseline technology cell costs in the Li-ion battery industry are about 2.5× the \$100-125/kWh ultimate target of the Department of Energy (DOE) Vehicle Technologies Office (VTO). In order to reach the target of a 2.5× increase in performance to 500 Wh/kg, novel R2R processing technologies will be required. Furthermore, polymer electrolyte fuel cell stacks currently cost almost 10× in low volumes compared to the ultimate cost of the DOE Fuel Cells Technology Office (FCTO) target of \$30/kW. Other examples of the Energy Efficiency and Renewable Energy (EERE) Office funded technologies that have a similar cost-target issue are chemical-process industry membranes, window films, photovoltaic (PV) films, and electronic films. The EERE Advanced Manufacturing Office (AMO) is poised to assist in reaching the low \$/m<sup>2</sup> costs of these various critical energy related applications through addressing R2R manufacturing problems common to each application.

## Preface

The following report provides the current status and technical accomplishments made during FY 2016 to overcome challenges for expanding use of R2R technologies and processing for enabling enhanced manufacturing of battery electrodes. This report documents the research conducted by four DOE national laboratories as a consortium in collaboration with industry partnerships to develop novel battery materials for improved energy storage applications. This research is directly applicable to advanced materials manufacturing strategies that apply a materials genome approach to enhance the performance of battery materials. This effort supports building the foundation of technologies, processes and a U.S. manufacturing base that will enable an order of magnitude in shorter process development cycles with the pathway for initial commercialization within months instead of years.

## Acknowledgements

First and foremost, the following scientists, investigators and technical support who are working diligently to realize their innovative ideas and technological developments in R2R processing and their desire to deploy them broadly for energy storage applications are acknowledged for their contributions:

**ANL:** Youngho Shin, Ozge Feridun, Andrew Jansen, Gerald Jeka, Alison Dunlop, Steve Trask, Bryant Polzin, Dennis Dees

**ORNL:** Marissa Wood, Jianlin Li

**NREL:** Peter Rupnowski, Tony Burrell, Brian Green, Guido Bender, Kyle Tangler, Nate Mitchell, Phil Clark, Bev Hiller, Dirk Decker, Kris Munch, Robert White, Bruce Bugbee, Joe Berry, Rob Tenent, Maikel van Hest

**LBNL:** Kenny Higa, Dula Parkinson, Harold Barnard, David Trebotich, Steve Ferreira, Gerd Ceder

We would like to acknowledge Matt Fronk, Delores Kruchten, Nancy Ferris, Daniel Ocorr, Andy Naukam, and Courtney Reich at Eastman Kodak, Rochester, NY, for their tour of their R2R facilities and their insights during a two-day technical workshop. Their inputs were of great value to the consortium team for building a technical portfolio, defining R2R problems and developing a work scope for FY 2017 and beyond.

Also, Greg Mullholland, Chief Operating Officer and Sean Paradiso at Citrine Informatics must be recognized for their collaboration and technical support with the analysis of the battery electrode research data and the development of a machine learning model for improving cathode design.

Finally, we would also like to acknowledge Fred Crowson, Energetics Incorporated, for his project management assistance and help in preparing and publishing this report.

This research at

- Oak Ridge National Laboratory, managed by UT Battelle, LLC for the U.S. Department of Energy, under contract DE-AC05-00OR22725
- Argonne National Laboratory, managed by UChicago Argonne, LLC for the U.S. Department of Energy, under contract DE-AC02-06CH11357
- Lawrence Berkeley National Laboratory, managed by University of California for the U.S. Department of Energy, under contract DE-AC02-05CH11231
- National Renewable Energy Laboratory, managed by Alliance for Sustainable Energy, LLC for the U.S. Department of Energy, under contract DE-AC36-08GO28308

was sponsored by the Office of Energy Efficiency and Renewable Energy, Advanced Manufacturing Office (Mark Johnson and David Hardy).

## Acronyms and Abbreviations

(Definitions for terminology used in this report are in the Glossary section at the end of this report)

°C	degrees Centigrade
μm	micrometers or microns
\$/kW	dollars per kilowatt
\$/m <sup>2</sup>	dollars per square meter
1C, 2C etc.	a charge current of 1, 2, etc. time the rated capacity
AC	alternating current
Ah	amp-hour
AMM	Advanced Materials Manufacturing
AMO	Advanced Manufacturing Office
ANL	Argonne National Laboratory
AOP	Annual Operating Plan
ASI	area specific impedance
BET	Brunauer, Emmett and Teller, a theory that aims to explain the physical adsorption of gas molecules on a solid surface
Bn	billion
C	chemical symbol for carbon
CA	California
CAMP	Argonne National Laboratory's Cell Analysis, Modeling and Prototyping facility
CB	carbon black
Chombo	Chombo is a set of tools for implementing finite difference and finite volume methods for the solution of partial differential equations on block-structured adaptively refined rectangular grids.
cm <sup>2</sup>	centimeter squared
Co	chemical symbol for cobalt
CO	Colorado
COMPRO	Software by Convergent Manufacturing Technologies for process analysis of complex structures
CPS	Corporate Planning System
CR2032	Designation for a button cell lithium battery rated at 3.0 volts
CRADA	Cooperative Research And Development Agreement
CVS	comma separated values
D10, D50, D90	the value of the particle diameter at 10%, 50% and 90% in the cumulative distribution for a group of particles
DC	District of Columbia
DOD	U.S. Department of Defense
DOE	U.S. Department of Energy
DP	dual pass; to process a coating on one side of a substrate on a single pass through a process and then coat the substrate on the back side of the substrate in a second pass
EC:DEC	ethylene carbonate (EC)–diethyl carbonate (DEC) electrolyte
EC:EMC	ethylene carbonate (EC)–ethyl methyl carbonate (EMC) electrolyte



EERE	Energy Efficiency and Renewable Energy
e.g.	abbreviation meaning “for example”; a Latin phrase, “ <i>exempli gratia</i> ” meaning “for the sake of example”
etc.	abbreviation for the Latin phrase “ <i>et cetera</i> ” which means “and so forth”
FCTO	Fuel Cells Technology Office
ft	foot or feet
ft/min	feet per minute
FY	fiscal year
g	gram or grams
Hg	chemical symbol mercury
HPPC	hybrid pulse-power capability (or characterization)
IL	Illinois
IR	infrared
kg	kilogram
Kodak	Eastman Kodak Business Park
kWh	kilowatt hour(s)
kWh/kg	killowatt hours per kilogram
L or l	liter(s)
LBNL	Lawrence Berkeley National Laboratory
Li	chemical symbol for lithium
LiPF <sub>6</sub>	Lithium hexafluorophosphate
M	molar
mAh	milliamp-hour
mAh/g	milliamp-hour per gram
MEA	membrane electrode assembly
MERF	Materials Engineering Research Facility
mg/cm <sup>2</sup>	milligram per square centimeter
min(s)	minute(s)
mm	millimeters
Mn	chemical symbol for manganese
MRL	Material Readiness Level
NCM or NMC	nickel-manganese-cobalt
NDE	nondestructive evaluation
Ni	chemical symbol for nickel
NMP	N-Methyl-2-pyrrolidone
N/P or N:P	concentration of conducting electrons to the electron hole concentration, i.e. , the negative to positive electrode ratio
NREL	National Renewable Energy Laboratory
NY	New York
OCP(V)	open circuit (or cell) potential (or voltage) - The potential of the working electrode relative to the reference electrode when no potential or current is being applied to the cell
OLED	organic light-emitting diode
ORNL	Oak Ridge National Laboratory

PE	polyethylene
PEMFC	proton exchange membrane fuel cell
pH	the negative logarithm of the effective hydrogen-ion concentration or hydrogen-ion activity in gram equivalents per liter of the solution
PIF	physical information file
PMD	PMD Inc., a systems integration company originally Pedavena Mold and Die Company)
PMI	Porous Materials, Inc.
PP	polypropylene
PSD	pore size distribution
Pt	chemical symbol for platinum
PV	photovoltaic
PVDF	polyvinylidene fluoride
QC	quality control
R2R	roll-to- roll
RPT	reference performance testing
S	second(s)
SEM	scanning electron microscope (or microscopy)
SiO	silicon oxide
SIMS	secondary ion mass spectrometry
SLC	A series designator for a natural flake graphite with surface treatment, spheroidal particle shape with low surface area, and various particle sizes used in batteries
SP	single pass
TN	Tennessee
TRL	Technology Readiness Level
TOF	time-of-flight (a technique used in microscopy)
TVR	Taylor Vortex Reactor
USABC	United States Advanced Battery Consortium
V	volt
vs.	versus
VTO	Vehicle Technologies Office
V/V	volume to volume ratio
Wh/kg	watt-hour per kilogram
wt%	percent by weight
XOS®	X-Ray Optical Systems, known as XOS®, is a leading manufacturer of application-specific X-ray analyzers
XRF	x-ray fluorescence (or fluorometer)



# Table of Contents

Foreword.....	iii
Preface.....	iv
Acknowledgements.....	v
Acronyms and Abbreviations.....	vi
List of Figures.....	x
List of Tables.....	xi
Roll-to-Roll Advanced Materials Manufacturing – DOE Laboratory Consortium.....	1
Abstract/Executive Summary.....	2
Accomplishments.....	2
Future Directions.....	3
Technology Assessment.....	5
Introduction.....	6
Approach.....	6
Results and Discussion.....	7
Collaboration/Coordination/Outreach.....	39
Challenges/Contingencies.....	40
Risks and Risk Handling.....	41
Technology Transfer Path.....	42
Conclusions.....	42
Glossary.....	45
References.....	51
Bibliography.....	52

# List of Figures

Figure 1. The 1L and 10L Taylor Vortex Reactors.....	9
Figure 2. A) Mix of 6/12 $\mu$ m particles, B) Single Pass 12 $\mu$ m Bottom/6 $\mu$ m Top, C) Single Pass 6 $\mu$ m Bottom/ 12 $\mu$ m Top.....	11
Figure 3. Cycle Life -Average Discharge Capacity (mAh/g of oxide material) versus cycle number for NCM 523 vs. graphite. This graph shows that there is a cell capacity dependence as a function of cycling rate. (3.0-4.2V).....	14
Figure 4. Average Coulombic Efficiency. Cycling efficiency of the cells and how it is changing over time. The graph is zoomed in on just the C/2 cycles. The data points for the C/20 cycle and HPPC are above and below this range, as expected. (3.0-4.2V).....	15
Figure 5. Average Discharge Capacity Retention of the various cathode architectures in full cells (vs. graphite). The 5th cycle in the Cycle Life test is taken as the 100% capacity marker. (3.0-4.2V).....	16
Figure 6. Capacity Fade in reference performance testing (RPT) cycle 1. Initial regression analysis of the battery lifetime dataset. The extracted charge capacities of three battery systems are plotted (symbols) as a function of time with a box-average and linear regression model shown to fit the data well.....	17
Figure 7. Predicted vs actual plots for electrochemical performance models a) charge capacity and b) discharge capacity.....	20
Figure 8. Predicted vs. actual performance plots for particle property models: a) TapDensity b) BET c) D10 d) D50 and e) D90.....	22
Figure 9. Rate performance comparison of pouch cells made with the six different cathode coatings. Each data point is an average of three pouch cells, with the initial capacity taken as the capacity at a discharge rate of C/10.....	27
Figure 10. a) First 100 cycles of a long-term pouch cell cycle life study. Charge C/3, discharge C/3. HPPC was performed every 50 cycles. b-d) HPPC results plotted as area specific impedance (Ohm-cm <sup>2</sup> ) before cycling (b), after 50 cycles (c), and after 100 cycles (d). Data is an average of 3 cells for each coating.....	28
Figure 11. a) First 800 cycles of a high rate pouch cell	

cycle life study. Charge 1C, Discharge 2C. HPPC was performed every 50 cycles. Each error bar is an average of the standard deviation for those 50 cycles. Data is an average of 2 cells for each coating (the 3rd cell in each coating series has not yet finished enough cycles to include). HPPC results plotted as area specific impedance (Ohm-cm <sup>2</sup> ) before cycling (b), after 200 cycles (c), after 400 cycles (d), and after 600 cycles (e). Data points in b) – e) without error bars represent only 1 cell.....	29
Figure 12. Comparison of capacity at C/10, C/2, and 2C discharge rates for ANL coin cells, ORNL coin cells, and ORNL pouch cells. ANL coin cells data is an average of 4 cells, ORNL coin cell data is an average of 3 cells, and ORNL pouch cell data is an average of 3 cells. a) Coating #1: All Small Particles (6 μm); b) Coating #2: Mixed Particles (6 μm & 12 μm); c) Coating #3: 2-Pass 12 μm Bottom/6 μm Top; d) Coating #4: 2-Pass 6 μm Bottom/12 μm Top; e) Coating #5: Dual Slot Die 12 μm Bottom/ 6 μm Top; f) Coating #6: Dual Slot Die 6 μm Bottom/12 μm Top.....	30
Figure 13a. Pore size distributions calculated from mercury porosimetry measurements of uncalendered (50-55% porosity) coatings.....	31
Figure 13b. Pore size distributions calculated from mercury porosimetry measurements of coatings calendered to 30% porosity.....	32
Figure 14. NREL web-line with the current porosity NDE configuration and conditions.....	33
Figure 15. Comparison of NREL porosity (top) and thermal data (bottom) for six electrode samples at 2 ft/min speed.....	34
Figure 16. XRF setup at NREL.....	35
Figure 17. XRF analysis of PEMFC and NMC electrodes.....	36
Figure 18. LBNL process flow for a predictive capability to accelerate materials adoption.....	37
Figure 19. Computer three-dimensional visualization of battery electrode material with NMC particles.....	37
Figure 20. Experimental setup for radiography of drying drop.....	38
Figure 21. Comparison of a droplet formed electrode material vs a R2R laminate electrode material (Top: Radiography image of drying NMC/CB/PVDF/NMP drop showing particle settling).....	39

Figure 22. Simulated discharge curves at two rates for half-cell with NMC electrode.....	39
--	----

Figure 23. Relationships of MRLs to System Milestones, TRLs, and Technical Reviews.....	47
---	----

## List of Tables

Table I. Preliminary 10L TVR synthesis run.....	10
---	----

Table II. Results of the rate study test from the 6 $\mu$ m and 12 $\mu$ m blended electrode at various porosities, tested in a coin half-cell (3.0-4.3V).....	12
--	----

Table III. Results of the formation and rate study test, the electrode architectures did not show a significant difference in performance (3.0-4.3V).....	12
---	----

Table IV. Negative to positive electrode ratio (N:P ratio) calculations for the Superior Graphite anode against the 40% porosity cathode architectures. The target value for the N:P ratio is 1.1-1.2.....	13
--	----

Table V. Screen shot of the matrix view of the data received from experimental collaborators at ANL.....	18
--	----

Table VI: Screen shot of the filter interface on the Citrination deployment.....	18
--	----

Table VII. Relative feature importance values as reported by the web interface. In this context, "prediction" refers to the Charge Capacity model.....	23
--	----

Table VIII. Percentage of total pores in different size ranges calculated from mercury porosimetry analysis of uncalendered (50-55% porosity) coatings.....	32
---	----

Table IX. Percentage of total pores in different size ranges calculated from mercury porosimetry analysis of coatings calendered to 30% porosity.....	32
---	----

Table X. Material Readiness Level Definitions.....	46
--	----

Table XI. Technology Readiness Level Definitions.....	49
---	----

# Roll-to-Roll Advanced Materials Manufacturing – DOE Laboratory Consortium

## **Claus Daniel, Project and Consortium Team Lead**

Oak Ridge National Laboratory (ORNL)  
Oak Ridge, TN 37831-6472  
Phone: (865) 946-1544  
Email: [danielc@ornl.gov](mailto:danielc@ornl.gov)

## **David L. Wood III, ORNL Project Team Lead**

Oak Ridge National Laboratory (ORNL)  
Oak Ridge, TN 37831-6472  
Phone: (865) 574-1157  
Email: [wooddl@ornl.gov](mailto:wooddl@ornl.gov)

## **Gregory K. Krumdick, ANL Project Team Lead**

Argonne National Laboratory (ANL)  
9700 S. Cass Avenue  
Building 362  
Argonne, IL 60439-4844  
Phone: (630) 252-3952  
Email: [gkrumdick@anl.gov](mailto:gkrumdick@anl.gov)

## **Michael Ulsh, NREL Project Team Lead**

National Renewable Energy Laboratory (NREL)  
15013 Denver West Parkway  
Golden, CO 80401  
Phone: (303) 275-3842  
Email: [Michael.Ulsh@nrel.gov](mailto:Michael.Ulsh@nrel.gov)

## **Venkat Srinivasan, LBNL Project Team Lead**

Lawrence Berkeley National Laboratory (LBNL)  
1 Cyclotron Road  
MS 70R 0108B  
Berkeley, CA-94720  
Phone: (510) 495-2679  
Email: [vsrinivasan@lbl.gov](mailto:vsrinivasan@lbl.gov)

## **David C. Hardy, DOE Roll-to-Roll Program Manager**

Department of Energy (DOE)  
Energy Efficiency and Renewable Energy (EERE)  
Advanced Manufacturing Office (AMO)  
1000 Independence Ave., S.W., Suite 5F-063  
Washington, DC 20585-0121  
Phone: (202) 586-8092  
E-mail: [david.hardy@ee.doe.gov](mailto:david.hardy@ee.doe.gov)

**Project Title/Corporate Planning System (CPS) Agreement Number:** Roll-to-Roll Manufacturing Science and Applications: From Ideal Materials to Real-World Devices/Oak Ridge National Laboratory CPS #31128, Argonne National Laboratory CPS #29915, National Renewable Energy Laboratory CPS #31128, Lawrence Berkeley National Laboratory CPS #25349

## Executive Summary

A DOE laboratory consortium comprised of ORNL, ANL, NREL and LBNL, coordinating with Kodak's Eastman Business Park (Kodak) and other selected industry partners, was formed to address enhancing battery electrode performance and R2R manufacturing challenges. The objective of the FY 2016 seed project was to develop a materials genome synthesis process amenable to R2R manufacturing and to provide modeling, simulation, processing, and manufacturing techniques that demonstrate the feasibility of process controls and scale-up potential for improved battery electrodes. [1] The research efforts were to predict and measure changes and results in electrode morphology and performance based on process condition changes; to evaluate mixed, active, particle size deposition and drying for novel electrode materials; and to model various process condition changes and the resulting morphology and electrode performance.

The four National Laboratories used a collaborative approach to look at compositions of materials with different particle sizes to make electrode samples using a R2R manufacturing process. The shape, size, and morphology of the materials, the chemistry of the formulation, the nature of slurries, their coating rate, the rate of drying all play a role in determining the final coating architecture, quality, and performance. A commercial cathode material was selected to make a series of electrodes by single pass, dual pass and slot die methods. Specific particle sizes of six micron (small) and twelve micron (large) were selected and slurries were prepared to make six variations of electrodes. The electrodes were configured to have all small particles (as a control), 50%/50% small and large particles, a combination of small particles in a top layer and larger particles in a bottom layer, and finally large particles in a top layer and small particles in a bottom layer. In this manner, the electrode could be varied to give porosities at 30%, 40% and 50%. Results from formation and rate studies of half-cell testing showed that porosity had little effect on the cell performance. Based on these results, a 40% porosity electrode was selected for further testing. The 40% porosity electrode also exhibits less curling than the 30% porosity for single-side coated electrodes making handling easier.

Rate study tests of the electrodes in a half-cell coin at 3.0-4.3V gave cell performance ranging from 148 to 177 mAh/g for C-rates of 2C to C/24. Formation and rate study cycle test results showed that the electrode architectures did not have a significant difference in performance at 3.0-4.3V for a reversible 1C rate of 150 to 155 mAh/g and for a reversible C/10 rate of 168 to 173 mAh/g, given an initial capacity of 189 to 194 mAh/g. Superior Graphite anodes were matched against the cathode materials and the N:P ratios were essentially the same (1.1 to 1.3) so a common anode material was used to evaluate the electrochemical performance of full coin cells. Tests of the cycle life average discharge capacity revealed that all of the available lithium in the system during each cycle was not utilized. Further exploration is needed to maximize the performance of the various cathode architectures.

Although there was slightly more variation in capacity between the different electrode coatings at higher discharge rates ( $\geq 1C$ ), performance measured for pouch cells was similar and all coatings exhibited a substantial drop in capacity (20-35% of initial C/10 discharge capacity) at a 2C discharge rate. There appears to be no significant difference in rate performance between the six cathode coatings; however, when coin cells were made using a different electrolyte, they showed improved performance at a 2C rate relative to the pouch cells, indicating that the different electrolyte may account for some difference in the rate performance. Mercury porosimetry characterization of the six calendered cathode coatings showed that all had similar pore size distributions which could also explain why there was little observed difference in the rate performance. Calendering of the coatings appeared to have some effect on preserving an advanced electrode architecture during high compression force.

An in-line x-ray fluorescence (XRF) system was set up and commissioned for non-destructive evaluation of coatings. The system was used for initial studies to understand the accuracy and sensitivity of the technique to battery cathode areal loading. Active thermography for real-time battery electrode porosity measurement, a technique that correlates a thermal measurement to porosity, was also explored. To conduct in-line porosity evaluations on a R2R web-line, cathode samples were spliced into a common roll, the spliced roll was run on a web-line under several test conditions, and thermal responses were measured. In-line porosity diagnostic measurements did not seem to be sensitive to the distinction between sequentially coated and simultaneously

coated (dual slot) layers, as was expected. However, the measurements did appear to be sensitive to the size and arrangement (in layers) of particles in the electrode material. Data from a run with all six electrodes at a line speed of 2 feet per minute showed consistent results across all six samples, i.e. small particles on top gives higher response. This inline porosity technique was also demonstrated on a separate coating line with as-coated active layers over a range of coating compositions, thicknesses, and process conditions including at line speeds up to 10 feet per minute. An existing porosity diagnostic model was modified to include a two or more layer construction of electrodes. This model was used to determine that the different particle sizes alone would not have caused the difference in a measured thermal response that was observed during active thermography measurements of the electrode samples. Scanning electron microscope images clearly show significant differences in surface structure between the electrodes with small particles in the top layer and those with large particles in the top layer, which is consistent with results obtained from the model. This could result in a change in surface reflectance and emissivity between samples. The model was modified and it was found that differences in emissivity and reflectance, based on the electrode surface structure, could definitely result in the differences in measured thermal responses that were observed.

The consortium team developed models for droplet studies, drying of slurries, and porosities of cathode materials in order to further the development of predictive capabilities for manufacturing processes that connect process variables to product performance. A system to accurately dispense microliters quantities of high-viscosity slurries was designed for droplet experiments. Data processing tools to reduce the influence of imaging artifacts required development. X-ray radiography was used to capture the evolution of the particles in a slurry to the formation of the electrode and the porosity was calculated starting at the bottom of the sample going to the top using tomography.

Tomography images showed that the viscosity clearly changes dynamics from a coffee ring to a frozen configuration. A viscous slurry showed similar thickness changes to R2R processed materials so this technique can be used to study process conditions. The modelling of the system resulted in similar behavior to the real R2R coatings within the first 50 microns. Simulated discharge curves for cell potential versus capacity at two rates for a half-cell revealed that the highest capacity was achieved at a 1C rate for the small particle size control sample. For the particle settling model, particle-particle and particle-wall interactions for a slurry drop packed with spherical particles were implemented. This included background fluid forces, both isotropic and rotational. The model also took into consideration the effects of particle dynamics in the settling process where clusters of larger particles tends to settle downward due to gravity, displacing some of the smaller particles, and moves the larger particles to a region where there are less particles.

The DOE laboratory consortium successfully completed all tasks on an accelerated schedule to develop an enhanced battery material using a R2R manufacturing process and to provide modeling, simulation, processing, and manufacturing techniques that demonstrate the feasibility and potential for scale-up. Technology transfer for this and other technology areas applicable to R2R manufacturing will begin in FY 2017 through a CRADA solicitation to industry and with a collaborative partnership with Kodak Eastman Business Park. This DOE-Industry partnership will result in low manufacturing costs, low energy processes, high volume production, high throughput due to thinner materials, compatibility with many material platforms, and products with varying sizes and dimensions. Technology alignment with DOE and consortium goals will be facilitated through the application of primary metrics of success, such as throughput, energy, and yield.

## Accomplishments

### ANL (Materials Synthesis, Device Evaluation and Data Mining)

- Established the capability to provide multiple kilogram quantities of custom cathode materials
- Provided kilogram samples of a commercial nickel-manganese-cobalt (NMC) cathode material
- Calendered multiple electrode samples to vary the porosity at 30%, 40% and 50% (as provided)
- Made coin cell half-cells and ran formation and rate study protocols to gather electrochemical data



- Analyzed electrochemical data to determine matching anode parameters for pouch cell evaluation
- Made full coin cells with the 40% porosity sample for electrochemical performance testing
- Obtained surface and cross-sectional scanning electron microscope (SEM) images on all cathode and matching anode electrodes
- Provided Citrine with material synthesis, analytical and electrochemical data for model development

#### **ORNL (Materials Processing, Materials Characterization, Device Assembly and Testing)**

- Formulated and coated a variety of multi-layer cathodes with different particle sizes and porosity gradients, and exchanged electrodes with other partner labs
- Completed six different cathode coatings of ~20-30 ft each using the ORNL pilot slot-die coater as a method for achieving bilayer electrode structure with mixed particle-size interface
- Initiated mercury (Hg) porosimetry for investigation of multi-modal pore-size distribution and time-of-flight secondary ion mass spectrometry (TOF-SIMS) for studying particle intermixing at the interfaces between individual electrode layers
- Constructed six 0.5-Ah pouch cells (three unit cells each) for each cathode coating using the matching anode made by ANL

#### **NREL (Morphology, Porosity and Metrology of Coatings)**

- Conducted porosity diagnostics on six ORNL electrode samples and performed data analysis
- Designed and fabricated enclosure for and mounted the x-ray fluorometer (XRF), initiated all safety and operations documentation and review, and performed operational validation and initial calibration
- Performed measurements of several NMC battery cathode and Pt/C proton exchange membrane fuel cell (PEMFC) electrode samples

#### **LBNL (Modeling and Simulation of Morphology and Performance Tomography of Dried Coatings)**

- Developed first ever radiography and tomography tool to visualize battery drying process.
- Developed a technique that demonstrates the ability to link process conditions to electrode structure which is the first step to process-structure-performance correlation for dilute versus concentrated slurries
- Initiated a physics-based model to describe the process during drying and included particle-to-particle interactions and fluid-particle forces
- Performed radiography-based droplet drying studies using a silicon oxide (SiO<sub>2</sub>)/conductive additive/carboxymethyl cellulose/water slurry as model of slurry drying, extracted particle concentration distribution from radiography data, and submitted a manuscript for review by *Journal of the Electrochemical Society*
- Developed a computational modeling framework to model particle suspensions in a slurry, simulating the settling of N microspheres in a solution due to gravitational and fluid forces. The framework is based on a suite of codes built on Chombo, a set of libraries that supports adaptive, finite volume numerical methods for partial differential equations
- Performed settling simulations of 6 micrometer (μm) and 12μm diameter particles

- Explored feasibility of droplet drying studies using current commercially-relevant NMC/conductive additive/ polyvinylidene fluoride (PVDF)/ N-Methyl-2-pyrrolidone (NMP) slurry, requiring development of a ventilation system and a tool for accurate dispensing of small volumes (microliters) of high-viscosity suspensions
- Performed x-ray micro-tomography on all electrode materials provided by ORNL
- Modified an existing electrochemical simulation of a half-cell containing an NMC electrode to incorporate the measurements obtained from the ORNL electrodes

## Future Directions

### Consortium Team

- Conduct research that will enable the U.S. to capture a substantial portion of a \$10Bn opportunity on membranes and flexible devices
- Integrate with and leverage solutions to DOE program offices specific applications whose technologies have matured to Technology Readiness Levels of TRL 5-7 (see the Glossary below for definitions of TRLs)
- Assess the problem of Material Readiness Level (MRL) 2-5 technologies in the core programs at national laboratories with an industrial CRADA program to move technologies to MRL 7 (see the Glossary below for definitions of MRLs)

### ANL

- Continue evaluation of battery electrode materials and data mining and model development with Citrine
- Evaluate the application of R2R processing to other technology areas beyond battery electrodes
- Investigate a battery electrode with a multilayer anode of varying porosity
- Assess the potential for membrane production for industrial cooling tower water descaling
- Investigate multi-layer Pt-skin nanoparticles/nanoframes for fuel cell applications
- Develop thick gradient anode electrodes to enhance charge rate
- Demonstrate a pilot scale process to provide low-energy and economically viable membranes for chemical purification/recovery and water desalination
- Investigate increasing the speed of resin wafer manufacturing and reducing labor costs through continuous process
- Evaluate a pilot-scale polymer-ceramic extruder capability for continuous manufacturing membrane films
- Demonstrate a capability to extrude and produce nanocomposite films with good dispersion of fillers for transparent film applications
- Evaluate the scalability of multilayer Pt-skin nanoparticles/nanoframes for fuel cell applications

### ORNL

- Retest rate capability and high-rate capacity fade of cathode Coatings 1-6 in separate sets of single-unit-cell pouch cells (~80 mAh size)

- Redesign cathode coatings exploring variations in calendering conditions that do not homogenize the six advanced electrode architecture designs
- Repeat similar coating test matrix for anode architecture optimization, as cells may be anode limited at these electrode loadings
- Evaluate anode materials processing and coatings and assess variations of graphite agglomerate morphology to re-evaluate the current cathode design
- Conduct TOF-SIMS analyses of interfaces at different depths of the electrode layers
- Assess low-cost methods of membrane electrode assembly manufacturing (slot-die, gravure, etc.) such as coating electrocatalyst layers onto gas diffusion media to make gas diffusion electrodes for polymer electrolyte fuel cells (PEFC)
- Evaluate R2R hot-pressing (calendering) of GDEs to polymer electrolyte membranes to make “unitized” MEAs
- Evaluate Manufacturing Demonstration Facility equipment (electron beam and laser fusing) for rapid prototyping of bipolar plate flow-field designs
- Assess implementation of new metrology methods (and methods proven in other industries) for MEA production QC (two-sided edge alignment, catalyst distribution, thickness control, adhesion strength, etc.)
- Explore advanced materials characterization parameters such as surface energy, capillary flow porosimetry (CFP), high resolution microscopy, etc.
- Assess the potential for integration of ORNL sensors, data analytics, and controls for manufacturing and analogous applications as they relate to DOE “Smart Manufacturing”
- Evaluate graphene oxide membranes for water treatment and ion separation

#### **NREL**

- Perform physical measurements of emissivity and thermal conductivity of the various cathode layers to augment the porosity model, making it applicable to a broader range of electrode structures
- Incorporate into the model and perform useful predictive analyses, including, for example, whether the general “thermal scanning” technique used for the porosity diagnostic can also be sensitive to loading
- Discuss the initial XRF data with ORNL (relative to their previous effort), determine a specific path forward, and complete further measurements to statistically evaluate the feasibility of the technique (and a particular device) for real-time cathode measurements
- Continue to share fully analyzed data with consortium partners
- Contribute to project planning, e.g. task details at the labs and planning for the industry solicitation, including the proposed additional funding from FCTO for fuel cell and hydrogen activities
- Develop an integrated data management and analysis pipeline to provide a data driven approach to manufacturing research that will leverage the existing NREL Laboratory Information Management System

#### **LBNL**

- Develop the first-ever large-scale database of synthesis of battery materials

- Collaborate with Brookhaven National Laboratory for reaction-pathway verification
- Develop visualization technique mimicking an R2R process
- Evaluate the effects of changing process conditions (particle size, viscosity, drying rate, multiple layers, water vs. NMP process)
- Apply colloidal science in developing physics based model for R2R process
- Provide additional details in the drying model

## Technology Assessment

Depending on the technology area of interest (batteries, fuel cells, membranes, etc.):

- Target: Increase throughput by 5x and reduce production footprint.
- Gap: Current baseline processes for battery materials are slow and require large areas for mass production.
- Target: Reduce energy consumption by 2x.
- Gap: New technologies are needed to enable new energy efficient devices and products that will reduce the nation's energy consumption and greenhouse gas emissions.
- Target: Increase production yield by 2x without increasing cost.
- Gap: Cell costs in the lithium (Li)-ion battery industry are about 2.5× the \$100-125/kWh ultimate target of DOE. In order to reach the target of a 2.5x increase in performance to 500 Wh/kg, novel R2R processing technologies will be required.
- Target: Enable substantial shift of manufacturing to the U.S. by assisting in the development of a domestic supply chain.
- Gap: The Brisk Insight report recommends the following: A standardized infrastructure needs to be established, parameters affecting defects control and throughput for various processes are required, pilot-line facilities for development and optimization of full processes are needed, and equipment and quality concerns need to be addressed.

## Introduction

Modern variants of proven, classical R2R coating technologies, as well as new coating methods, are needed for enabling widespread commercialization of renewable energy storage and conversion technologies. Established coating methods, such as multi-layer slot-die, gravure, reverse comma, tape casting, etc. with homogeneity and uniformity superior to spraying methods need to be further adapted for improving performance of electrochemical energy storage and conversion, electrolytic hydrogen production, smart flexible sensors for building energy efficiency improvement, flexible displays such as organic light emitting diodes (OLEDs) and electronics, and photovoltaic panels. The shape, size, and morphology of the materials, the chemistry of the formulation, the nature of slurries, their coating rate, the rate of drying etc. all play a role in determining the final coating architecture, quality, and performance. In addition, non-destructive evaluation (NDE) of the produced coatings for improving in-line quality control (QC) and identification of defects, prior

to down-stream value added steps being performed, is of paramount importance. These projects brought together expertise from four national laboratories to solve the complex nature of the R2R process.

## Approach

The R2R AMM DOE Consortium Team effort was initiated and funded in April 2016 as a seed project to produce a battery electrode with enhanced performance using a R2R process and various compositions of NMC material. The project was accelerated in order to obtain meaningful results by the end of FY 2016 (approximately seven months). Even with this short schedule, ALL milestones were met.

The FY 2016 project included tasks to identify specific particle sizes of NMC electrode material, prepare slurries and electrode coatings, determine the areal weights of the coatings, prepare coatings for matching anodes, conduct porosity diagnostics, make operational an XRF system for inline metrology studies, conduct x-ray tomography of cathode samples, conduct characterization studies of the coating materials, and conduct device testing for rate capability, AC impedance, and initial capacity fade. Additionally, the team would develop models for droplet studies, drying of slurries, and porosity diagnostics of two or more layers of cathode materials. All data from this effort and similar projects funded by the VTO and FCTO would be provided to Citrine who would examine a wide range of pertinent electrochemical testing data and characteristic performance and life data to determine which adjustable parameters most strongly influence performance and life. They would also conduct an analysis of material synthesis process data and cell performance to determine synthesis conditions for optimizing material, chemical and electrochemical performance. A project schedule was formulated for an accelerated effort by the consortium team and all of the FY 2016 milestones were met.

The objective for this project was to look at novel materials of different particle sizes that could be used to make electrode samples with a R2R manufacturing process that would have improved performance over current battery technologies. Each of the four national laboratories were assigned tasks that could achieve the positive results in a collaborative manner.

ANL identified large and small particle sizes of commercial NMC material and sent one kilogram samples to ORNL to form electrode materials using a R2R process. ANL would form cathodes using the same materials and conduct porosity studies on both ORNL and ANL samples. They would also perform anode matching and cell testing and provide all results to the other labs and to Citrine for data mining, which would assist with design optimization. ANL monitored the data mining and materials process model development efforts by Citrine. Citrine also analyzed material synthesis process data and cell performance data to determine synthesis conditions for optimizing material, chemical and electrochemical performance.

ORNL prepared slurries and coating materials for six different cathodes with the following deposition variations: 100 wt% small particles (control), 50/50 mixed small and large particles in a single coat, dual pass with large particles first and then small particles, dual pass with small particles first and then large particles, single pass dual slot die with large particles on bottom and small on top, and single pass dual slot die with small particles on bottom and large on top. The areal weights for each of the coatings were checked and coatings were prepared for matching anodes. Electrode samples were sent to NREL for porosity studies and to ANL and LBNL for performance studies and modelling efforts. The intent was to be able to predict and understand the morphology and determine the performance of all electrode materials made with a R2R process.

NREL conducted coating characterization studies and quality control development. This included performing porosity diagnostics and installing and operating an XRF system to obtain data that would allow modifying an existing porosity diagnostic model to include a two-layer electrode construction. NREL then utilized the modified model for sensitivity analyses and update original porosity data, which would be provided to the other national laboratories.

LBNL performed modeling, simulation and droplet model studies on the cathode samples from ORNL and using data from NREL and ANL. The droplet model study compared porosity gradients in the model to the actual R2R electrodes received from ORNL. X-ray tomography was used to conduct these analyses. LBNL developed a preliminary model of the electrode drying process and determined the ability of model to predict changes with changing particle size. The results from this micro-structure model were then compared to experimental rate data on large particles and small particles.

## Results and Discussion

### ANL

The long-term goal of this project is to extend the Materials Engineering Research Facility (MERF) efforts to focus on advanced materials engineering and synthesis for R2R applications to ensure acceleration of, and not just discovery of, new materials but also their adoption in R2R applications. The MERF would leverage the Citrine datamining tool to enable optimal manufacturability of the materials. The objective of this task is to conduct process scale-up and synthesis of new materials. Advanced materials developed for R2R manufacturing will be synthesized in larger batches with a high degree of reproducibility. Materials produced will be provided to Argonne's Cell Analysis, Modeling and Prototyping (CAMP) facility for early feasibility roll-processing work. It is an integrated team designed to support production of prototype cells using semi-automated cell fabrication equipment, and includes activities in materials validation, modeling, and diagnostics. Citrine's datamining tool will be evaluated and performance data will be provided to refine the model.

### *MERF Summary*

In FY 2016, the MERF was tasked to establish additional synthesis capabilities specifically for AMO programs, leveraging existing equipment. To accomplish this, a new 10L Laminar Taylor Vortex Reactor (TVR) was installed to complement an existing 1L TVR (see Figure 1) and additional Nabertherm calcination furnaces were installed to expand the existing capability. Preliminary run produced 600g of metal oxide cathode materials and a subsequent run produced over one kilogram of material. This equipment is now available for the kilogram-scale production of co-precipitated metal oxide particles. The results for a preliminary 10L TVR synthesis run are given in Table I.

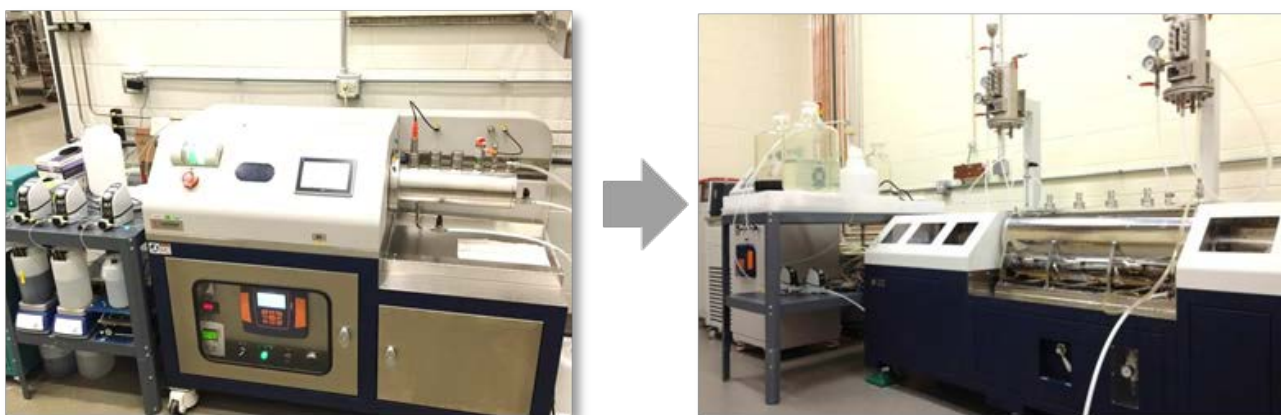
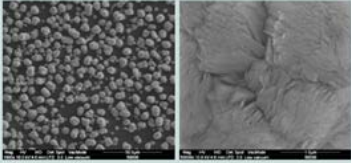
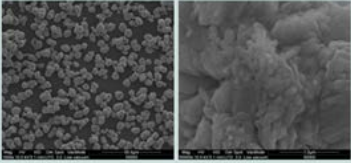


Figure 1. The 1L and 10L Taylor Vortex Reactors

Table I. Preliminary 10L TVR synthesis run

	pH & temperature of co-precipitation reaction	Cathodes calcined using $\text{Li}_2\text{CO}_3$	Cathode calcined using $\text{LiOH}\cdot\text{H}_2\text{O}$
	11.8(@50°C)	800°C	800°C
Scale, rotation	10 liters, 1250rpm ~600g	34g	35g
ICP	$\text{Ni}_{0.506}\text{Co}_{0.200}\text{Mn}_{0.294}(\text{OH})_2$	$\text{Li}_{1.06}\text{Ni}_{0.505}\text{Co}_{0.200}\text{Mn}_{0.295}(\text{OH})_2$	$\text{Li}_{1.05}\text{Ni}_{0.505}\text{Co}_{0.200}\text{Mn}_{0.295}(\text{OH})_2$
TD, g/cc	1.91	2.21	2.25
PSA, $\mu\text{m}$	4.11 / 7.29 / 12.57	4.16 / 7.01 / 12.01	4.49 / 7.89 / 14.12
BET, $\text{m}^2/\text{g}$	5.80	0.49	0.52
SEM			
Rate tests	-	Rate tests (CAMP protocols) will be conducted in half-coins @ 30°C	

Equipment was ordered at the start of this program; however, due to long equipment lead times, it was decided to initiate the collaboration using commercially available cathode materials. Small (6 $\mu\text{m}$ ) and large (12 $\mu\text{m}$ ) NCM 523 cathode particles were identified. Three commercial cathode powder samples were provided to ORNL and one to LBNL by CAMP.

### ***CAMP Summary***

In FY 2016, ANL's CAMP facility was tasked to evaluate various cathode architecture electrodes that were produced by ORNL. After the evaluation of the cathodes, the CAMP facility was tasked to produce an anode electrode that matched the cathodes and supply them to ORNL to fabricate pouch cells. Lastly, the CAMP facility (with the help of the MERF) performed full cell testing of the various cathode architectures in coin cells. The CAMP facility used their own testing protocol, based upon the U.S. Advanced Battery Consortium (USABC) testing protocol for electric vehicles to evaluate the various systems. The following sections describe this work and the results.

### ***Half-Cell Evaluation of Various Cathode Architectures***

Six cathode architectures were supplied to the CAMP facility from ORNL. These electrode architectures are:

- 1) 6 $\mu\text{m}$  NCM 523 only
- 2) 6 $\mu\text{m}$  /12 $\mu\text{m}$  NCM 523 blended
- 3) Dual Pass: 6 $\mu\text{m}$  Bottom Layer/ 12 $\mu\text{m}$  Top Layer
- 4) Dual Pass: 12 $\mu\text{m}$  Bottom Layer/ 6 $\mu\text{m}$  Top Layer
- 5) Single Pass: 12 $\mu\text{m}$  Bottom Layer/ 6 $\mu\text{m}$  Top Layer
- 6) Single Pass: 6 $\mu\text{m}$  Bottom Layer/ 12 $\mu\text{m}$  Top Layer

To examine the differences in these architectures, the MERF took SEM images of all of the electrodes. Figure 2 highlights the cross section of the blended electrodes and the two different single pass architectures.



These are the most interesting images of the various electrode architectures. These images show how ORNL changed the architecture of the electrode to enhance the performance.

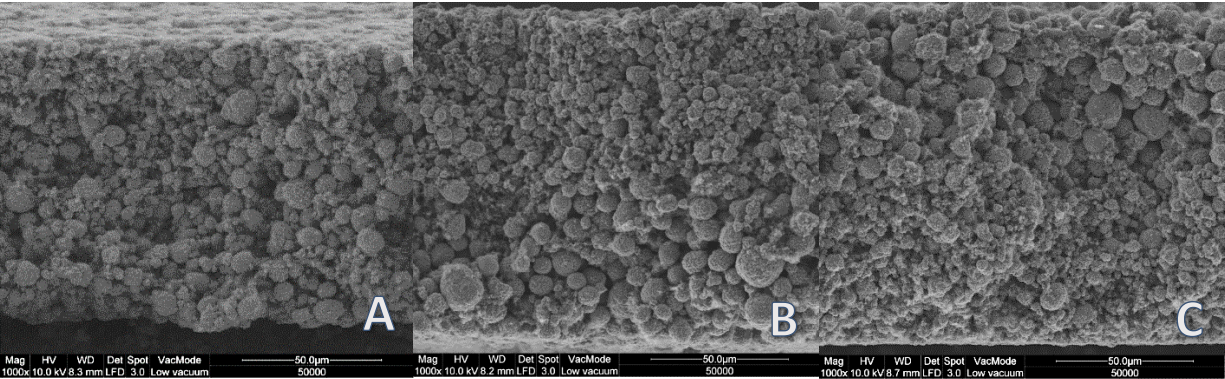


Figure 2. A) Mix of 6/12 $\mu$ m particles, B) Single Pass 12 $\mu$ m Bottom/ 6 $\mu$ m Top, C) Single Pass 6 $\mu$ m Bottom/ 12 $\mu$ m Top

To evaluate the electrochemical performance of these electrodes, several data points were collected. These data points are initial capacity, reversible C/10 rate capacity, and reversible 1C rate capacity. To collect this data, half-cell coin cells (CR2032) were made with the cathodes provided and a Li metal anode. The separator used for these cells was Celgard 2325 and the electrolyte used was 1.2M LiPF<sub>6</sub> in EC:EMC (3:7 wt%). The electrochemical testing was done in two steps: 1) Formation Cycling (3 cycles at C/10 rate) and 2) Rate Study Cycling (2 cycles at C/20, 3 @ C/10, 3@C/5, 3@C/3, 3@C/2, 3@1C, and 3@2C) to collect the required data. (The discharging rates for C/2 and faster used a C/3 charging rate) For all of these half-cell tests, a voltage window of 3.0 to 4.3V was used.

On top of the architecture, the effects of porosity on the cathodes was evaluated to see if the performance changes for electrodes of over 115 $\mu$  in thickness. Three porosities were evaluated: ~50%, ~40% and ~30%. The results from the half-cells at these various porosities showed that the porosity had little effect on the cell performance through the Formation and Rate Study cycles. Table II shows a sample data set from one electrode at various porosities. Based upon these data, CAMP recommended a 40% porosity cathode electrode for further testing. The 40% porosity electrode also exhibits less curling than the 30% porosity for single side coated electrodes, making handling easier. If double side electrodes are to be used in the future, a 30% porosity could be achieved and still have a usable electrode. This would line up with what industry is currently doing.

Table II. Results of the rate study test from the 6 $\mu$ m and 12 $\mu$ m blended electrode at various porosities, tested in a coin half-cell (3.0-4.3V)

C-rate	6/12 Micron Blend Electrode 30% Porosity mAh/g	6/12 Micron Blend Electrode 40% Porosity mAh/g	6/12 Micron Blend Electrode 50% Porosity mAh/g
2C	131	148	147
1C	152	153	153
C/2	163	158	158
C/5	170	165	165
C/10	172	170	170
C/24	173	177	176

Examining the six different cathode architectures through the Formation and Rate Study cycles also showed very little differences between the architectures. Table III shows the data collected from the various cathode electrodes. The data collected from this testing was then used to create a graphite anode that was capacity matched to the six different cathodes.

Table III. Results of the formation and rate study test, the electrode architectures did not show a significant difference in performance (3.0-4.3V)

Electrode (40% Porosity)	Initial Capacity mAh/g	Reversible C/10 Rate Capacity mAh/g	Reversible 1C Rate Capacity mAh/g
6 micron Only	192	173	150
6/12 micron Blended	194	170	153
<b>Dual Pass:</b> 6 um bottom/ 12 um top	191	170	154
<b>Dual Pass:</b> 12 um bottom/ 6 um top	189	169	154
<b>Single Pass:</b> 12 um bottom/ 6 um top	190	168	153
<b>Single Pass:</b> 6 um bottom/ 12 um top	192	170	155

#### *Matching of Anode to Cathode Electrodes*

Previous evaluation of Superior Graphite SLC1520P graphite powder yielded the necessary data in order to design a matching anode to the ORNL cathodes. The data collected on the SLC1520P graphite is as follows: initial capacity = 365 mAh/g, reversible C/10 rate capacity = 330 mAh/g and reversible 1C rate capacity =

320 mAh/g. Using this data and the data from Table III, a single anode could be designed to work with all six of the ORNL cathodes and still achieve an acceptable negative to positive electrode ratio (N:P ratio). An ideal case for an N:P ratio is between 1.1-1.2. In this case, the N:P ratio was calculated using several cycling rates to make sure the cells were in the desired N:P range under various cycling conditions. With these calculations, CAMP determined an ideal anode loading to target. The anode that was fabricated in the CAMP facility was: 91.83 wt% Superior Graphite SLC1520P graphite, 2 wt% Timcal C45 carbon black, 6 wt% Kureha 9300 PVDF and 0.17 wt% oxalic acid. The copper foil used was 10 $\mu$  thick. The total electrode thickness was 116 $\mu$  (106 $\mu$  thick electrode thickness – single side). The porosity was 33.2% and the total coating loading was 15.36 mg/cm<sup>2</sup>. The density of this electrode is 1.45 g/cm<sup>3</sup>. Table IV shows the N:P ratios of the anode with the various cathode architectures. To provide context on the cathodes used in this work, the loadings ranged from 24.07 to 26.64 mg/cm<sup>2</sup> loading and a total electrode thickness (electrode + foil) range of 115 to 121 $\mu$  at ~40% porosity.

Table IV. Negative to positive electrode ratio (N:P ratio) calculations for the Superior Graphite anode against the 40% porosity cathode architectures. The target value for the N:P ratio is 1.1-1.2.

Electrode (40% Porosity)	Neg 1 <sup>st</sup> Cycle/ Pos 1 <sup>st</sup> Cycle	(Rev Neg- (PIRC-NIRC))/ Rev Pos at ~C/10	(Rev Neg- (PIRC-NIRC))/ Rev Pos at ~1C
6 micron Only	1.16	1.18	1.31
6/12 micron Blended	1.20	1.22	1.32
<b>Dual Pass:</b> 6 um bottom/ 12 um top	1.10	1.11	1.19
<b>Dual Pass:</b> 12 um bottom/ 6 um top	1.22	1.24	1.32
<b>Single Pass:</b> 12 um bottom/ 6 um top	1.14	1.16	1.24
<b>Single Pass:</b> 6 um bottom/ 12 um top	1.13	1.15	1.22

#### Full Cell Evaluation of Electrodes

After developing matched anode and cathode electrodes, full coin cells were made to evaluate the electrochemical performance of the systems. Again in this case Celgard 2325 separator was used along with the 1.2M LiPF<sub>6</sub> in EC:EMC (3:7 wt%). These cells underwent the following testing protocols; 1) Formation, 2) Rate Study, 3) hybrid pulse-power capability (HPPC) (3C Discharge; 2.25C Charge), and 4) Cycle Life. The voltage window used in this testing was 3.0-4.2V. Protocols 1-3 are defined as characterization testing. These tests provide the initial data on the cells to ensure that the performance is good and none of the cells are doing anything out of the normal. If all the data looked good in these test, they were moved onto the Cycle Life testing. In the Cycle Life testing, a single C/20 cycle was done, then 47 cycles at C/2 rate and then an HPPC test was performed. This test block was repeated four times. All of the six cathode architecture cells looked good through the characterization protocol and all cells were moved onto the Cycle Life testing. At the time of this report, all the cells have completed their first Cycle Life testing (>250 cycles). Figure 3 shows the average capacity vs cycle number for all of the cells being tested. In this graph, it is possible to see the effects of the cycling rate on available capacity in the cell. In the Cycle Life protocol, there is a C/20 cycle that is showing what capacity is actually available in the cell. In these cases, there is much more

capacity available in the cell at C/20 then at the C/2 rate. The C/20 rate causes the uptick in the capacity every 47 cycles.

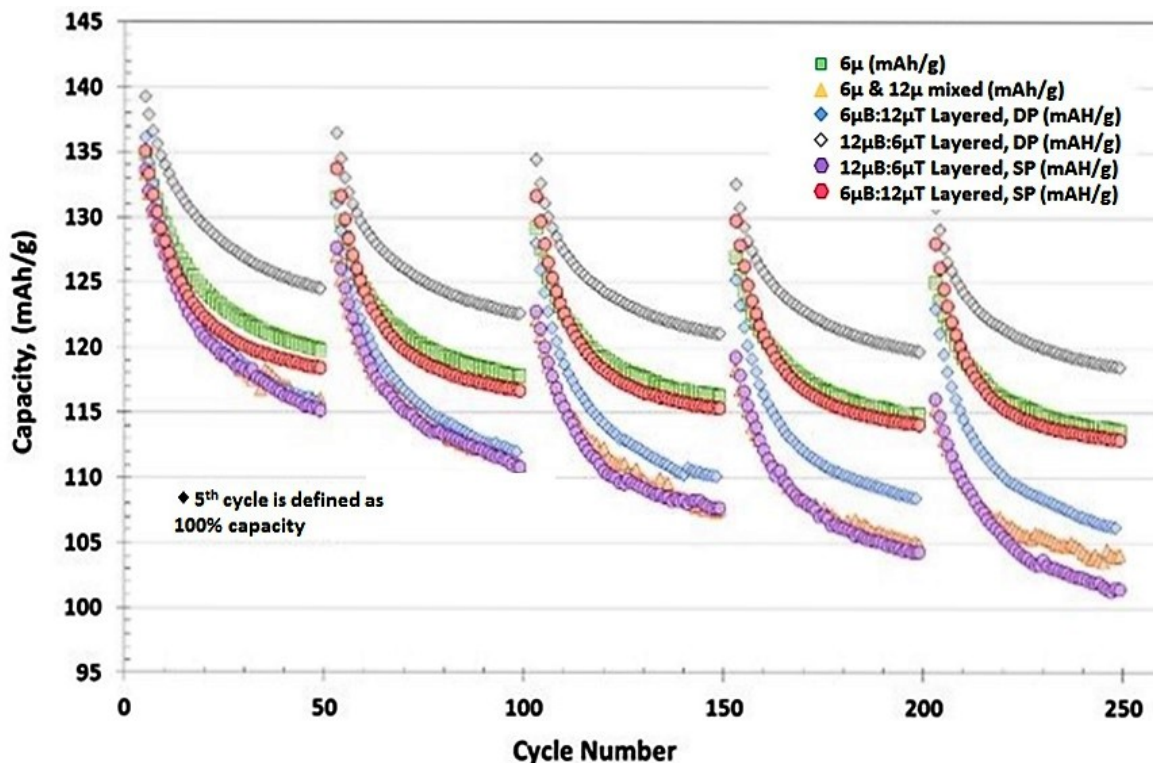


Figure 3. Cycle Life -Average Discharge Capacity (mAh/g of oxide material) versus cycle number for NCM 523 vs. graphite. This graph shows that there is a cell capacity dependence as a function of cycling rate. (3.0-4.2V)

To understand why the capacity is going down during the C/2 cycling, Figure 4 examines the cycling efficiency of each of the cathode architectures. With all of these cells, a Cycling Efficiency in the mid 90% range is observed. This means that all of the available Li in the system during each cycle was not assessed. The Li is getting trapped on one side of the cell at faster rates. The slow rate moves the Li where it needs to be. Further exploration is needed to maximize the performance of the various cathode architectures.

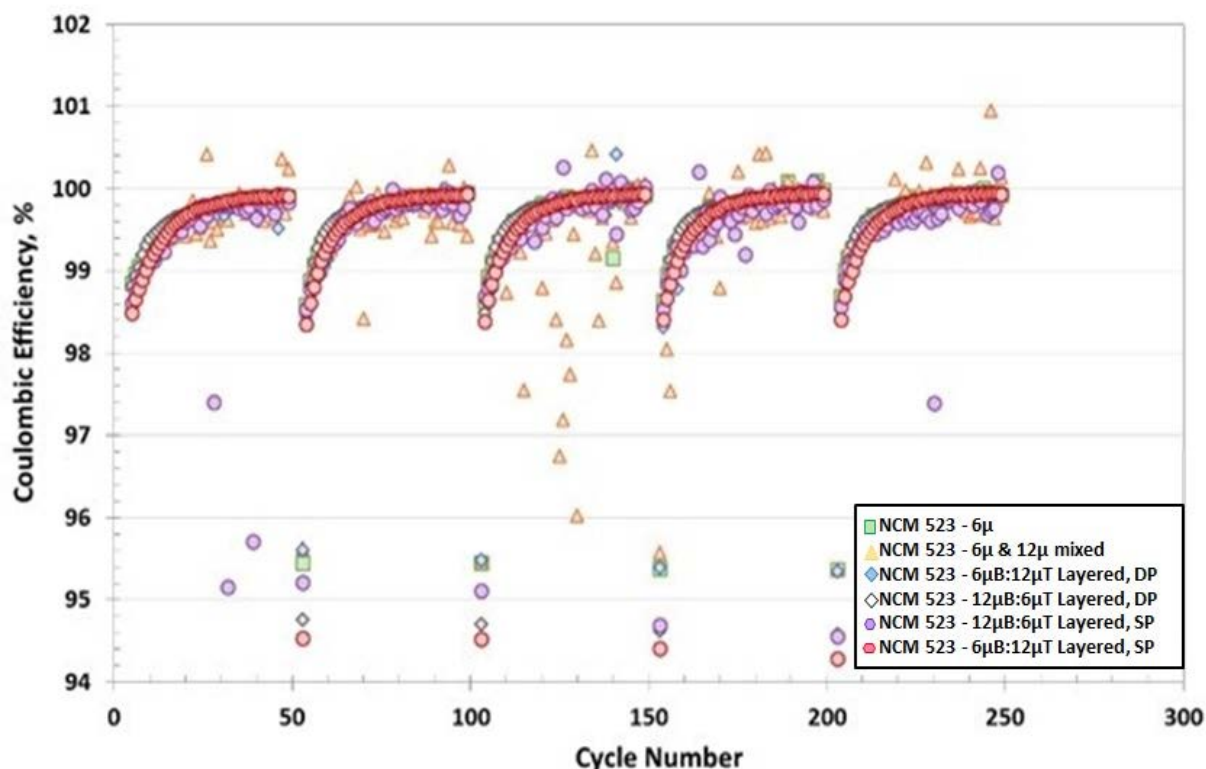


Figure 4. Average Coulombic Efficiency. Cycling efficiency of the cells and how it is changing over time. The graph is zoomed in on just the C/2 cycles. The data points for the C/20 cycle and HPPC are above and below this range, as expected. (3.0-4.2V)

Lastly, Figure 5 shows the capacity retention for each of the systems. Testing is still ongoing, at the time of this report. Figure 5 shows that some of the cathode architectures are performing better than others. From the data the Double Pass 12μB:6μT was the best performing cells so far, but close behind were the 6μ only cells and the Single Pass 6μB:12μT cells. The other cells showed a lower capacity retention and were grouped together. The Double Pass 6μB:12μT cells and the 6μ and 12μ Blended cells were about the same and the Single Pass 12μB:6μT was lowest performing so far. With this data, no specific trends can be determined as to what cathode architecture works the best. Further testing and analysis is needed to fully understand the cathode architecture and how to design the electrode that will take advantage of the electrode structure.



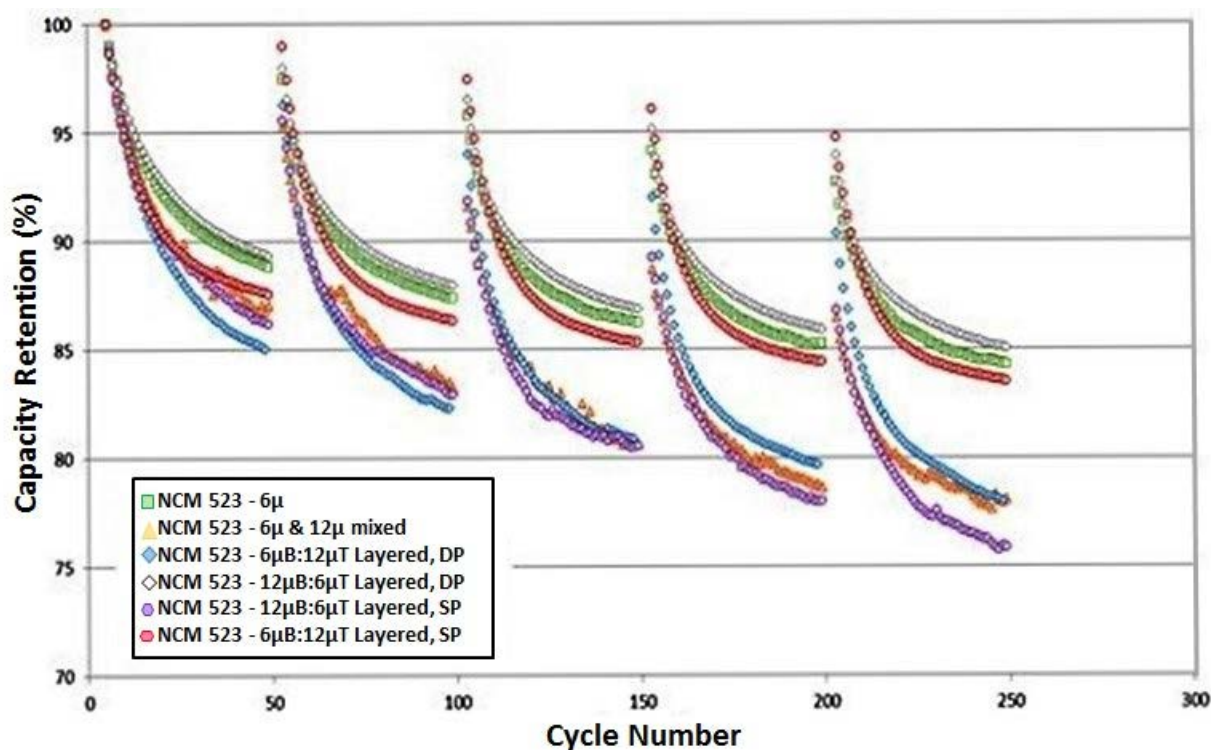


Figure 5. Average Discharge Capacity Retention of the various cathode architectures in full cells (vs. graphite). The 5<sup>th</sup> cycle in the Cycle Life test is taken as the 100% capacity marker. (3.0-4.2V)

### Citrine Summary

Argonne established a subcontract with Citrine for materials data mining program development and provided Citrine with sample datasets. Citrine is currently summarizing material synthesis, chemical and electrochemical analysis data.

#### *Characterization of Li-ion performance and life data - Examine database of electrochemical data*

Argonne provided Citrine with 1758 documents containing performance measurements over the lifetime of several battery chemistries subjected to a variety of load and storage conditions. These documents are broadly heterogeneous in their structure and internal formatting. Citrine has developed tools to extract the performance data as a time-series of voltage and current, and derived quantities such as capacity and energy. Data was tagged with contextual information, such as temperature date of collection, and aggregated across samples with the same target chemistry.

As a first-pass, Citrine fitted linear regression models to the decay of capacity and energy measured at each reported over loading conditions. In doing so, Citrine cleaned the data to reduce variance and discard outliers. An example of the resulting fit can be seen in Figure 6, which was derived from the "EPT2011042" data set. The results of this fit was consistent with Argonne's pre-existing understanding of the data, validating the extraction and cleaning process.

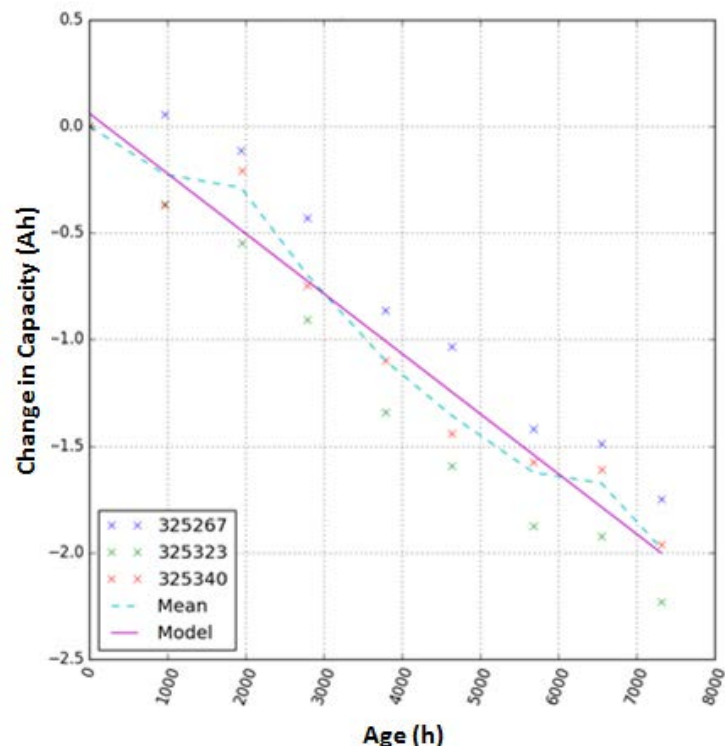


Figure 6. Capacity Fade in reference performance testing (RPT) cycle 1. Initial regression analysis of the battery lifetime dataset. The extracted charge capacities of three battery systems are plotted (symbols) as a function of time with a box-average and linear regression model shown to fit the data well.

#### *Apply advanced analytics to determine performance sensitivity on adjustable parameters*

Citrine selected advanced analytic methods to evaluate the data. First, the time-series data for voltage and current was featurized using a combination of traditional techniques, such as curve fitting, and unsupervised machine learning, such as principle component analysis, to supplement sample-specific contextual information. The combination of contextual and time-series-derived features will be used as inputs to supervised machine learning techniques, such as random forests, to predict performance and lifetime measures, such as capacity decay rate. The predictiveness of these models will be evaluated via cross-validation.

The models chosen provide a notion of "feature importance", i.e., the sensitivity of the model prediction to an input. These can be used to evaluate the sensitivity of the performance of the battery on its adjustable parameters, which is desired to achieve battery optimization. The feature items of importance and predictive models will be incorporated into a report at the end of the task.

#### *Battery Material and Cell Performance Modeling - Data ingested and made available to researchers*

Citrine completed ingestion and structuring of the electrochemical cell data obtained from the team at ANL. In order to accomplish this, Citrine established a file exchange mechanism to allow researchers at ANL to easily convert their data from CSV (comma separated values) to the PIF (physical information file) format that the Citration platform expects. In addition, a file converter was deployed to the platform to facilitate continuous incorporation of new data into the models as they become available.



The database has been made available through a custom deployment of the Citrination platform at <https://emery.citrination.com>. One of the primary motivations behind storing data in the PIF format is the flexibility to store hierarchical information in a way that respects common material property relationships. Any structured information, such as measurement conditions attached to properties or contextual information about the instruments used, is preserved in the PIF view (accessible via the View link shown in Table V below).

Table V. Screen shot of the matrix view of the data received from experimental collaborators at ANL

GeneralPlots

SHOW FILTERSTOGGLE COLUMNSENABLE ALLDISABLE ALLEXPORT TO CSV

	Processing										Reactant Solution		
Record	Reactor Type	Reactor Capacity	Batch or Continuous	Target Residence Time	Length of Reaction	Room Temperature	Reaction Temperature	Reactor pH	Sample pH	Stir Speed	TM molarity	NaOH molarity	NH4 molarity
<a href="#">View</a>	Batch	20 L	Batch	20 hr	20 hr	294.15 K	320.350 K	11.12	12.08	1000 RPM	2.4 mol/L	0.8 mol/L	2.4 mol/L
<a href="#">View</a>	Batch	20 L	Batch	20 hr	20 hr	294.15 K	321.15 K	10.3	10.99	1000 RPM	1.33333 mol/L	1.33333 mol/L	1.33333 mol/L
<a href="#">View</a>	Batch	20 L	Batch	20 hr	20 hr	294.15 K	321.050 K	10.99	11.81	1000 RPM	1.33333 mol/L	1.33333 mol/L	1.33333 mol/L
<a href="#">View</a>	Batch	20 L	Batch	20 hr	20 hr	294.15 K	320.65 K	10.7	11.55	1000 RPM	2.4 mol/L	0.8 mol/L	2.4 mol/L

Typically, however, researchers are interested in a tabular view of the data, defined by applying a relational schema to the PIFs indexed on the site. Here, the original comma separated value (CSV) view is displayed, but the deployment is configurable and can display almost any relational representation of the data a user requests. The data here can be searched and subsampled using an intuitive filter interface as shown in Table VI. The filters allow researchers to ask simple questions of their data before interrogating the models.

Table VI: Screen shot of the filter interface on the Citration deployment

Filters

SEARCH

CLEAR ALL FILTERS

HIDE

General

Show

EXPORT TO CSV

Composition

Show

Processing

Hide

Reactor Type

ON

✓ TVR

Batch

Reaction Temperature

OFF

Reactor pH

OFF

Sample pH

OFF

Stir Speed

OFF

Reactant Solution

Show

Cathode Analytical Data

Show

Room Temperature	Reaction Temperature	Reactor pH	Sample pH	Stir Speed	TM molarity	NaOH molarity	NH <sub>4</sub> molarity	D10	D50
294.15 K	320.350 K	11.12	12.08	1000 RPM	2.4 mol/L	0.8 mol/L	2.4 mol/L	2.8911 μm	5.2506 μm
294.15 K	321.15 K	10.3	10.99	1000 RPM	1.33333 mol/L	1.33333 mol/L	1.33333 mol/L	3.1979 μm	5.5353 μm
294.15 K	321.050 K	10.99	11.81	1000 RPM	1.33333 mol/L	1.33333 mol/L	1.33333 mol/L	2.4051 μm	4.016 μm
294.15 K	320.65 K	10.7	11.55	1000 RPM	2.4 mol/L	0.8 mol/L	2.4 mol/L	2.9182 μm	4.8637 μm
294.15 K	321.15 K	10	10.69	1000 RPM	1.33333 mol/L	1.33333 mol/L	1.33333 mol/L	3.1824 μm	5.7091 μm

### *Material models built and cross-validated*

Citrine's data scientists assembled a pair of coupled models that captures the full battery cell development process from electrode particle synthesis to electrochemical performance. The flow of information in this system naturally proceeds from the reactor conditions used to generate the precursor solution from which the electrode particles are grown to the cell performance. Often the case in experimental systems, especially at early stages of development, the amount of data available is much too small to use in a strictly data mining capacity. In this context, Citrine's approach was to model the system in a physically motivated way that respects the known relationships between variables. Electrochemical performance is a direct expression of available active surface area, particle pore tortuosity, surface chemistry, electrolyte, and many other features of the composed system. Directly trying to connect reaction conditions to electrochemical performance puts an unnecessary burden on the machine learning system. Practically speaking, this burden ultimately expresses itself as a need for much larger amounts of data in order to build accurate models. Instead, Citrine reduced the process into a simple two-model cascade.

Beginning with particle synthesis, experimental degrees of freedom were collected including reactor type (Taylor Vortex vs. Batch), conditions (pH, temperature, stir speed), and chemistry to build a model mapping reactor conditions to particle properties (size distribution, tap density, and specific surface area). This model can be used in isolation in order to identify key degrees of freedom governing particle morphology (as described by the predicted quantities such as D10, D50, D90 and Brunauer, Emmett and Teller (BET) results) or to transform experimental degrees of freedom into predicted particle properties that can be used as inputs to the second model. Once the particle characterization is known (or inferred from reactor conditions), values are entered into a model that is built to map these properties to the observed electrochemical performance properties of interest (first charge and discharge capacities). The website contains information about each of these models on the model report page accessible at the following address:

<https://emery.citration.com/status/learning>.

There, the performance can be evaluated on the basis of the cross validated predicted vs actual plots, an industry standard for measuring the generalizability of the trained models. These plots, reproduced below, were generated by splitting the available data into two pieces: 90% for training and 10% for testing. Once the data was sampled (without replacement) to generate these two data sets, models are trained on the training split, then used to make predictions on the holdout test set. The predicted property values were then plotted against the actual values in order to gain some insight into how well the models perform on unseen data. A perfect model would express a predicted vs. actual curve that falls exactly on the  $y=x$  line, whereas a completely naïve model would deviate substantially for values far from the mean. The electrochemical property performance plots (charge and discharge capacity) are provided in Figure 7. These demonstrate fairly strong performance despite the limited amount of data available (24 unique sets of experimental conditions). The intermediate models used to predict particle properties, such as TapDensity, specific surface area (BET) and particle size distributions of D10, D50, and D90 as a function of reactor conditions are shown in Figure 8.

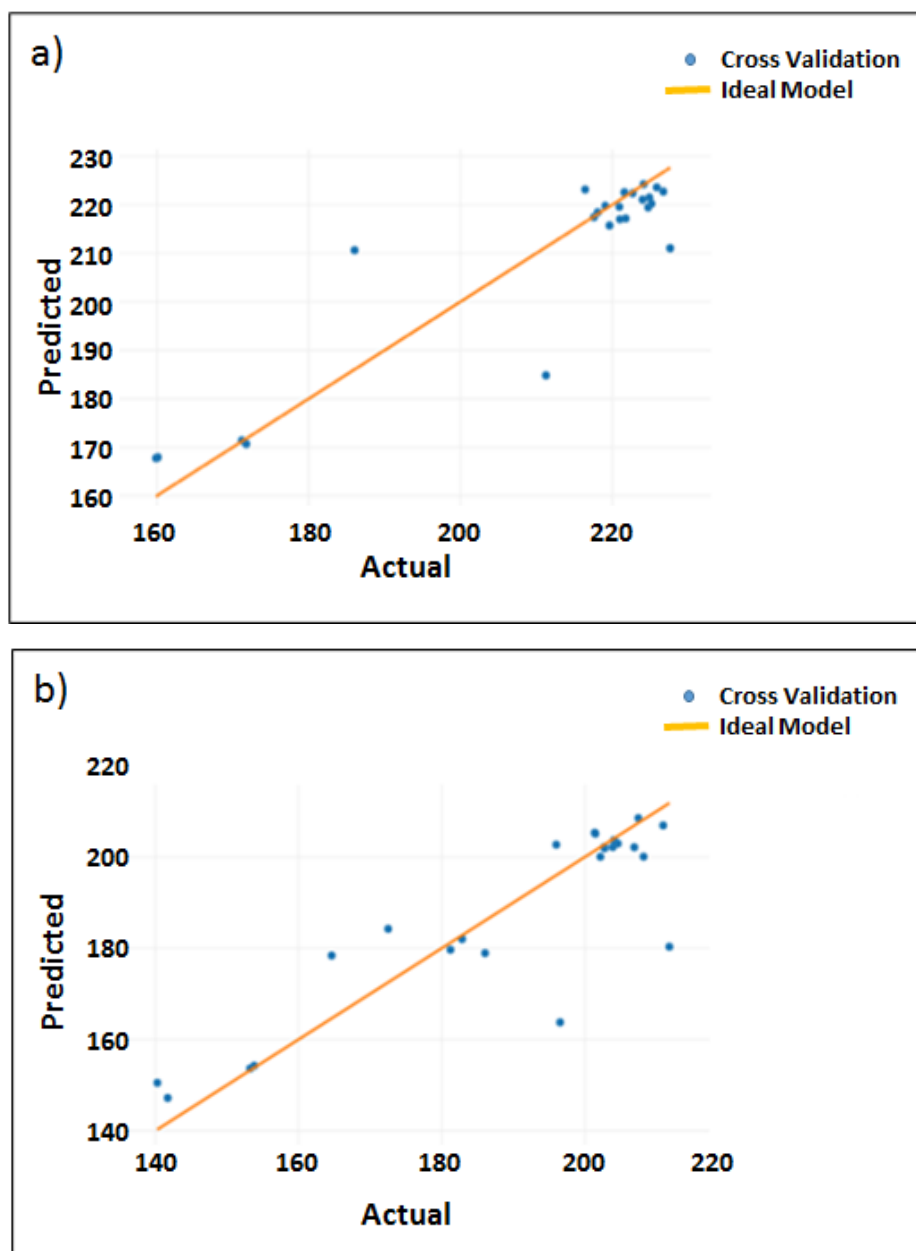
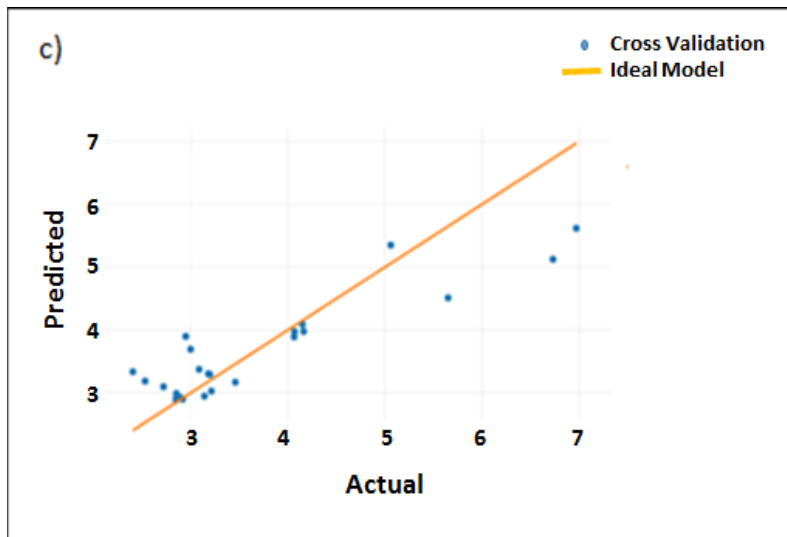
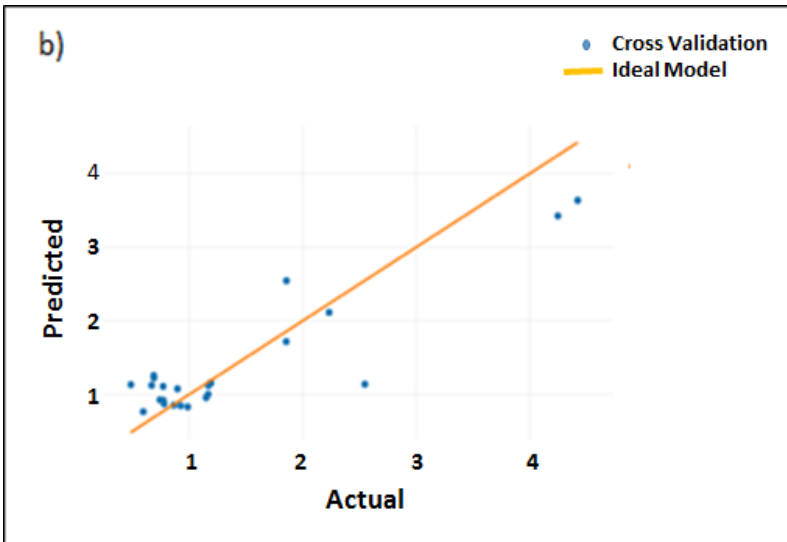
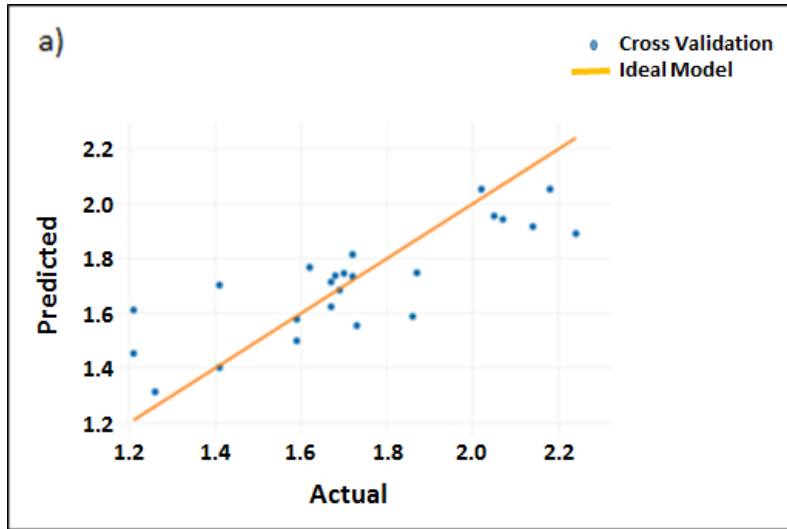


Figure 7. Predicted vs actual plots for electrochemical performance models a) charge capacity and b) discharge capacity



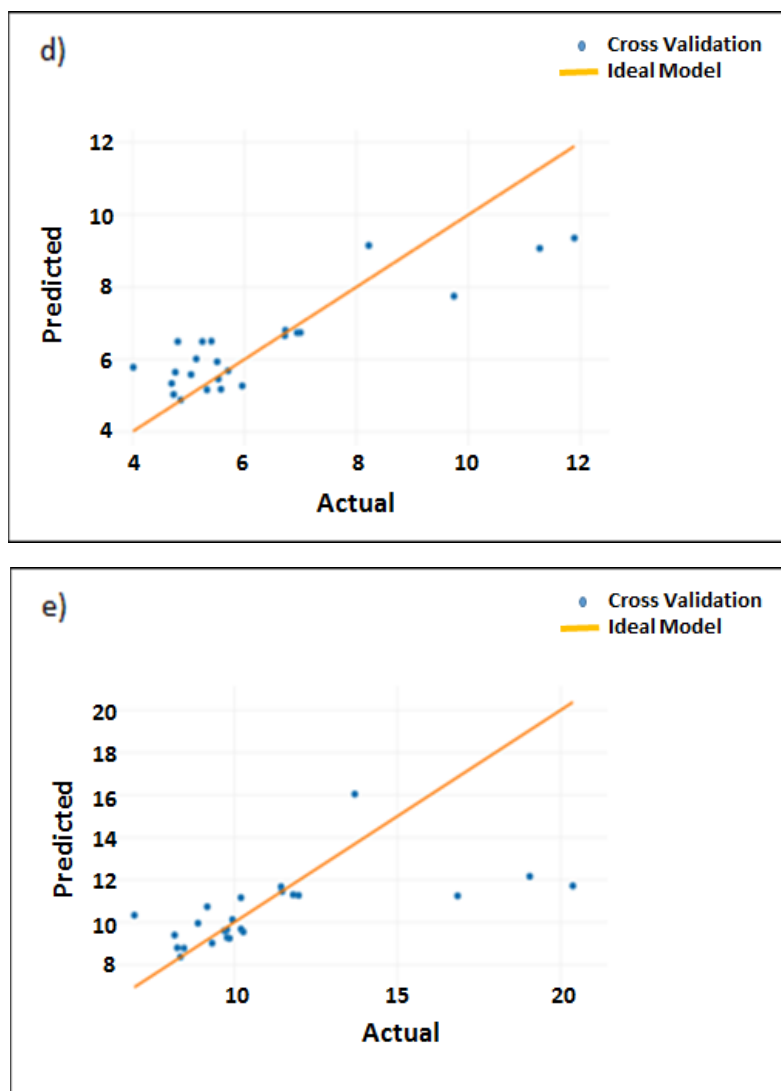


Figure 8. Predicted vs. actual performance plots for particle property models: a) TapDensity b) BET c) D10 d) D50 and e) D90

The models report page also provides information about the relative predictive power of the different features. These importance values are derived from the relative information gained by selecting a given feature over the others when attempting to group points in the dataset. Table VII contains the list of relative importance values for the inputs to the charge capacity model. The BET in Figure 2b is by far the most important feature, followed by target manganese (Mn) and nickel (Ni) content. Surprisingly, the particle size distribution does not appear to have a strong impact on the predicted capacity. Finally, the models were made available via a prediction interface that can be accessed at <https://emery.citrination.com/batteries/predictions>. This interface offers users immediate feedback on new ideas before heading back into the lab.

Table VII. Relative feature importance values as reported by the web interface. In this context, "prediction" refers to the Charge Capacity model.

prediction	
predicted_BET	0.4758612508219944
Mn	0.17110940633888627
Ni	0.1505306934403797
predicted_D90	0.051048861700581386
predicted_TapDensity	0.04262631193572887
predicted_D50	0.037394438445596735
Co	0.03610771839773985
predicted_D10	0.03532131891909287

## ORNL

### *Cathode Coatings*

ORNL initially constructed Li-ion cathode coatings with varying electrode architectures. Six different cathode coatings of ~20-30 ft each were completed using the ORNL pilot slot-die coater. These coatings contained various combinations of two different NMC 532 particle sizes (~ 6  $\mu\text{m}$  and ~12  $\mu\text{m}$ ) to help correlate processing conditions with final microstructure and electrochemical performance. All six coatings have similar areal loadings to enable direct comparisons. The first four coatings were completed using a single slot die, while the last two were achieved using a dual slot die, which allows two wet layers of different particle compositions to be coated on top of each other simultaneously. The thickness and areal loading of each coating was measured after drying, and samples of each were sent to ANL, NREL, and LBNL for further analysis, the most time sensitive of which is ANL testing to determine appropriate anode loadings for optimized full cell N/P balancing.

For pouch cell testing, six 0.5-Ah pouch cells (three unit cells each) were constructed at ORNL for each cathode coating using the matching anode made by ANL. All cathodes were calendered to ~35% porosity, and all pouch cells were filled with 1.2 M  $\text{LiPF}_6$  in 3:7 (v/v) EC/DEC. Three pouch cells from each coating were used for rate performance testing, while the other three were used for cycle life (capacity fade) studies. All cells underwent the following test protocol:

- **Formation (2.5V to 4.2V):** 4 Cycles at Charge C/20, Discharge C/20
- **Rate Capability (2.5V to 4.2V):**
  - 5 Cycles at Charge C/5, Discharge C/10
  - 5 Cycles at Charge C/5, Discharge C/5

- 5 Cycles at Charge C/5, Discharge C/3
- 5 Cycles at Charge C/5, Discharge C/2
- 5 Cycles at Charge C/5, Discharge 1C
- 5 Cycles at Charge C/5, Discharge 2C
- 5 Cycles at Charge C/5, Discharge 3C
- 5 Cycles at Charge C/5, Discharge 5C
- 5 Cycles at Charge C/5, Discharge 9C or 10C (Depending on total cell capacity and current limit of instrument)

High-rate capacity fade testing was performed at 1C/2C on the pouch cells that were subjected to rate performance testing (i.e. these cells already had experienced 45 cycles before the beginning of the life testing). These cells were cycled according to the following protocol after the rate performance testing was completed:

- **Cycle Life (2.5V to 4.2V):** 1000 Cycles at Charge 1C, Discharge 2C with HPPC every 50 cycles
- **HPPC (2.5V to 4.2V):** Charge C/3; 9 pulses: Discharge 10% of capacity at C/3; Discharge 2C for 10 s, Charge 1.5C for 10 s

The first cathode coating contained only the small particle size in order to serve as a control, while the second coating contained a mixture of small and large particle sizes (50/50 wt%). The composition of each slurry is given below, along with the final thickness and areal loading of each finished coating.

**Coating 1: 100% Small Particle Size Coating (Control)**

90 wt% Toda NMC 532 Small Particles (~6  $\mu\text{m}$ )  
 5 wt% Denka Carbon Black  
 5 wt% Solvay 5130 PVDF

Total Electrode Thickness: 140  $\mu\text{m}$   
 Al Foil Thickness: 15  $\mu\text{m}$   
 Coating Thickness: 125  $\mu\text{m}$   
 Areal Loading (of coating only): 25.04  $\text{mg}/\text{cm}^2$

**Coating 2: Mixed Small & Large Particle Sizes (50/50 wt%)**

45 wt% Toda NMC 532 Small Particles (~6  $\mu\text{m}$ )  
 45 wt% Toda NMC 532 Large Particles (~12  $\mu\text{m}$ )  
 5 wt% Denka Carbon Black  
 5 wt% Solvay 5130 PVDF

Total Electrode Thickness: 134  $\mu\text{m}$   
 Al Foil Thickness: 15  $\mu\text{m}$   
 Coating Thickness: 119  $\mu\text{m}$   
 Areal Loading (of coating only): 24.72  $\text{mg}/\text{cm}^2$

The next two cathode coatings were completed using a two-step process in which one layer was coated and dried first before a second layer was coated on top of it. Coating 3 consists of a large particle size layer on the bottom next to the current collector and a small particle size layer on the top, while Coating 4 has the opposite configuration. In each case, the thickness and areal loading of the bottom layer was first measured separately before adding the top layer and measuring the final coating. These values are given below, along with the composition of each slurry.

**Coating 3: Two Pass**

**Bottom Layer: Large Particle Size | Top Layer: Small Particle Size**

*Bottom layer slurry:*



90 wt% Toda NMC 532 Large Particles (~12  $\mu\text{m}$ )  
5 wt% Denka Carbon Black  
5 wt% Solvay 5130 PVDF

*Top layer slurry:*

90 wt% Toda NMC 532 Small Particles (~6  $\mu\text{m}$ )  
5 wt% Denka Carbon Black  
5 wt% Solvay 5130 PVDF

Total Electrode Thickness: 130  $\mu\text{m}$   
Al Foil Thickness: 15  $\mu\text{m}$   
Total Coating Thickness: 115  $\mu\text{m}$   
Bottom Layer Thickness (Large particle coating only): 65  $\mu\text{m}$   
Top Layer Thickness (Small particle coating only): 50  $\mu\text{m}$

Total Areal Loading (of coating only): 24.29  $\text{mg}/\text{cm}^2$   
Bottom Layer Areal Loading (Large particle coating only): 12.49  $\text{mg}/\text{cm}^2$   
Top Layer Areal Loading (Small particle coating only): 11.80  $\text{mg}/\text{cm}^2$

**Coating 4: Two Pass**

**Bottom Layer: Small Particles | Top Layer: Large Particles**

*Bottom Layer Slurry:*

90 wt% Toda NMC 532 Small Particles (~6  $\mu\text{m}$ )  
5 wt% Denka Carbon Black  
5 wt% Solvay 5130 PVDF

*Top Layer Slurry:*

90 wt% Toda NMC 532 Large Particles (~12  $\mu\text{m}$ )  
5 wt% Denka Carbon Black  
5 wt% Solvay 5130 PVDF

Total Electrode Thickness: 144  $\mu\text{m}$   
Al Foil Thickness: 15  $\mu\text{m}$   
Total Coating Thickness: 129  $\mu\text{m}$   
Bottom Layer Thickness (Small particle coating only): 68  $\mu\text{m}$   
Top Layer Thickness (Large particle coating only): 61  $\mu\text{m}$

Total Areal Loading (of coating only): 26.64  $\text{mg}/\text{cm}^2$   
Bottom Layer Areal Loading (Small particle coating only): 13.08  $\text{mg}/\text{cm}^2$   
Top Layer Areal Loading (Large particle coating only): 13.56  $\text{mg}/\text{cm}^2$

The last two coatings have the same compositions as Coatings 3 and 4 but were completed using the dual slot die, which allowed two wet layers to be coated on top of each other simultaneously (rather than coating a wet layer on top of a dry bottom layer). Coating 5 consists of a large particle size layer on the bottom next to the current collector and a small particle size layer on the top, while Coating 6 has the opposite configuration. For each coating, the bottom and top layers were first run separately in order to estimate what the areal loading of each layer would be in the finished coating. The thickness and areal loading of the finished coating was then measured. These values are given below, along with the composition of each slurry.

**Coating 5: Dual Slot Die**

Bottom Layer: Large Particle Size | Top Layer: Small Particle Size

*Bottom layer slurry:*

90 wt% Toda NMC 532 Large Particles (~12  $\mu\text{m}$ )  
5 wt% Denka Carbon Black  
5 wt% Solvay 5130 PVDF

*Top layer slurry:*

90 wt% Toda NMC 532 Small Particles (~6  $\mu\text{m}$ )  
5 wt% Denka Carbon Black  
5 wt% Solvay 5130 PVDF  
Total Electrode Thickness: 143  $\mu\text{m}$   
Al Foil Thickness: 15  $\mu\text{m}$   
Total Coating Thickness: 128  $\mu\text{m}$   
Total Areal Loading (of coating only): 25.75  $\text{mg}/\text{cm}^2$

**Coating 6: Dual Slot Die**

**Bottom Layer: Small Particles | Top Layer: Large Particles**

*Bottom Layer Slurry:*

90 wt% Toda NMC 532 Small Particles (~6  $\mu\text{m}$ )  
5 wt% Denka Carbon Black  
5 wt% Solvay 5130 PVDF

*Top Layer Slurry:*

90 wt% Toda NMC 532 Large Particles (~12  $\mu\text{m}$ )  
5 wt% Denka Carbon Black  
5 wt% Solvay 5130 PVDF

Total Electrode Thickness: 143  $\mu\text{m}$   
Al Foil Thickness: 15  $\mu\text{m}$   
Coating Thickness: 128  $\mu\text{m}$   
Total Areal Loading (of coating only): 25.75  $\text{mg}/\text{cm}^2$

***Pouch Cell Testing***

The rate performance results are shown in Figure 9, and results were almost identical for all six coatings at discharge rates  $<1\text{C}$ . Although there was slightly more variation in capacity between the different coatings at higher discharge rates ( $\geq 1\text{C}$ ), performance was similar within a  $2\sigma$  error range, with all coatings showing a substantial drop in capacity (down to 20-35% of initial C/10 discharge capacity) at a 2C discharge rate. Consequently, it is concluded that there is no significant difference in rate performance between these particular cathode coatings.

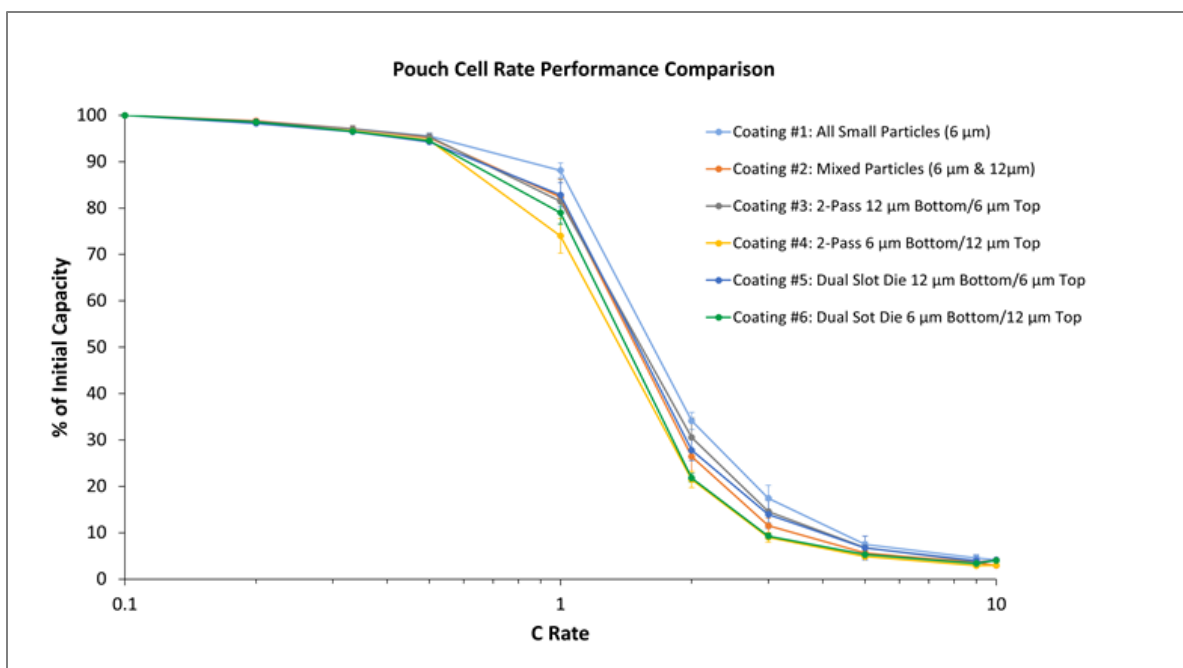


Figure 9. Rate performance comparison of pouch cells made with the six different cathode coatings. Each data point is an average of three pouch cells, with the initial capacity taken as the capacity at a discharge rate of C/10.

The capacity fade study is still in the early stages, and these cells are still running. Capacity retention to date, which includes results from the first 100 cycles for each coating, is plotted in Figure 10a. No significant difference was observed in capacity fade after 100 cycles at 0.33C/-0.33C charge/discharge rates between cells made with the six different cathode coatings. The HPPC test results before cycling, after 50 cycles, and after 100 cycles are shown in Figure 10b-d. Interestingly, the area specific impedance (ASI) of cells made with Coating #6 (Dual slot die, 6 μm bottom/12 μm top) was found to be higher than for those made with the other five coatings. However, the ASI of the cells made with the other five coatings was similar and did not show much change after the first 100 cycles. These findings are consistent with the electrode designs themselves, in that a larger difference between designs would be expected at the higher rate cycling of 1C/-2C, given that the bilayer architectures are supposed to help with mass-transport limitations during high-rate discharging.

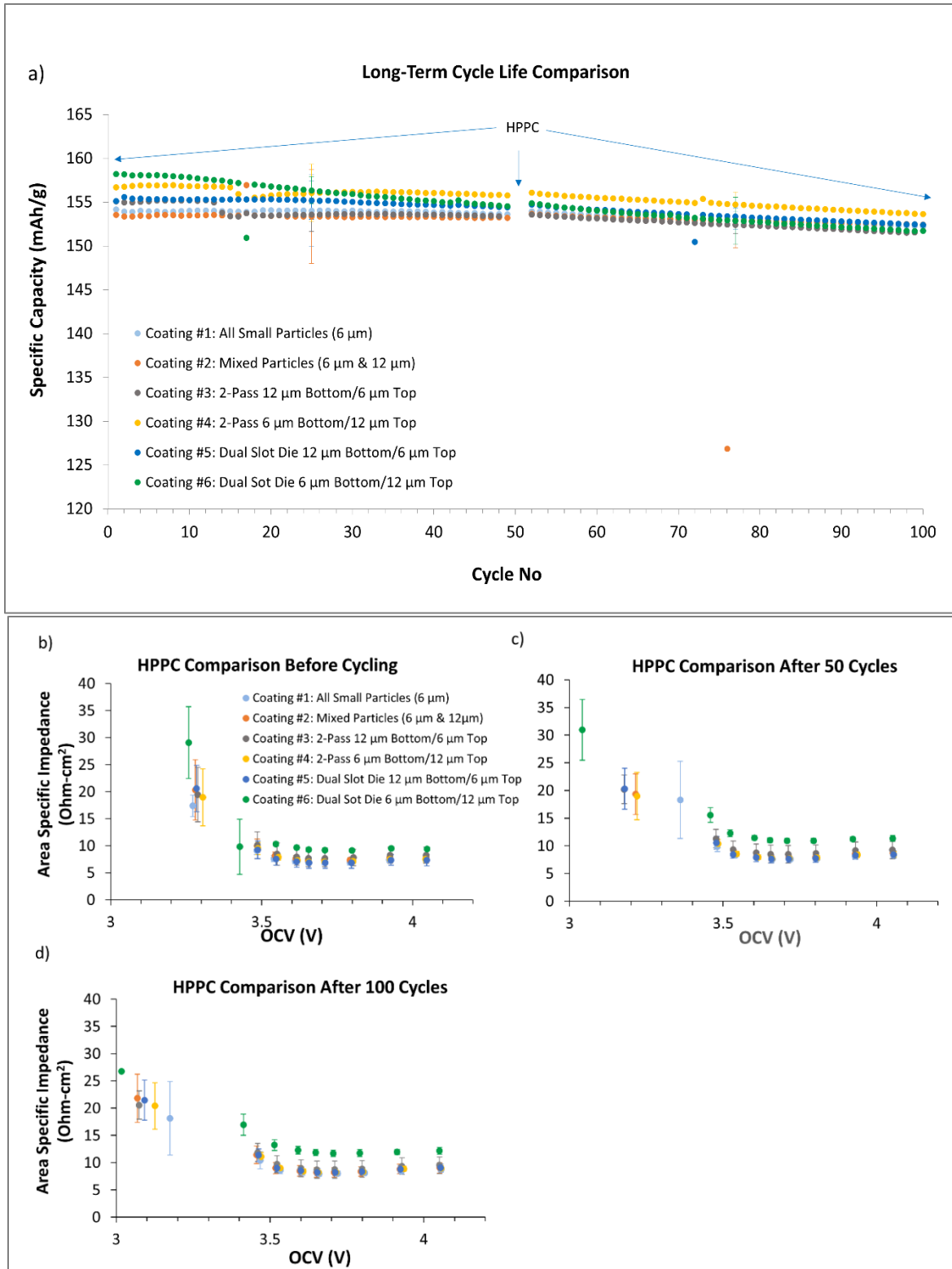


Figure 10. a) First 100 cycles of a long-term pouch cell cycle life study. Charge C/3, discharge C/3. HPPC was performed every 50 cycles. b-d) HPPC results plotted as area specific impedance (Ohm-cm<sup>2</sup>) before cycling (b), after 50 cycles (c), and after 100 cycles (d). Data is an average of 3 cells for each coating.

Figure 11 shows the capacity of pouch cells made with each coating through 800 high-rate cycles. HPPC results before cycling and after 200, 400, and 600 cycles are shown in Figure 11b-e. The capacity of all of the cells is low at 2C discharge rates, and there is quite a bit of variation between cells made from the same coating. There is little difference in the capacity retention or ASI between any of the pouch cells when cycled at 1C/-2C, but all cells showed a slightly higher ASI after cycling. It can be concluded, however, that Coatings 1-3, which include the two baselines with all small particles and mixed particle sizes, outperformed Coatings 4-6 after 800 cycles. A surprising finding was that Coating 3 (two-pass with small particles on top) significantly outperformed Coating 5 (dual slot-die with small particles on top), as it was expected that the interfacial contact resistance of Coating 3 (with one dried layer on top of the other) would cause prohibitive ohmic losses during high-rate cycling. Therefore, the cathode architectures investigated in this study need further optimization and understanding in terms of the full effects of particle size, porosity gradient, and coating process.

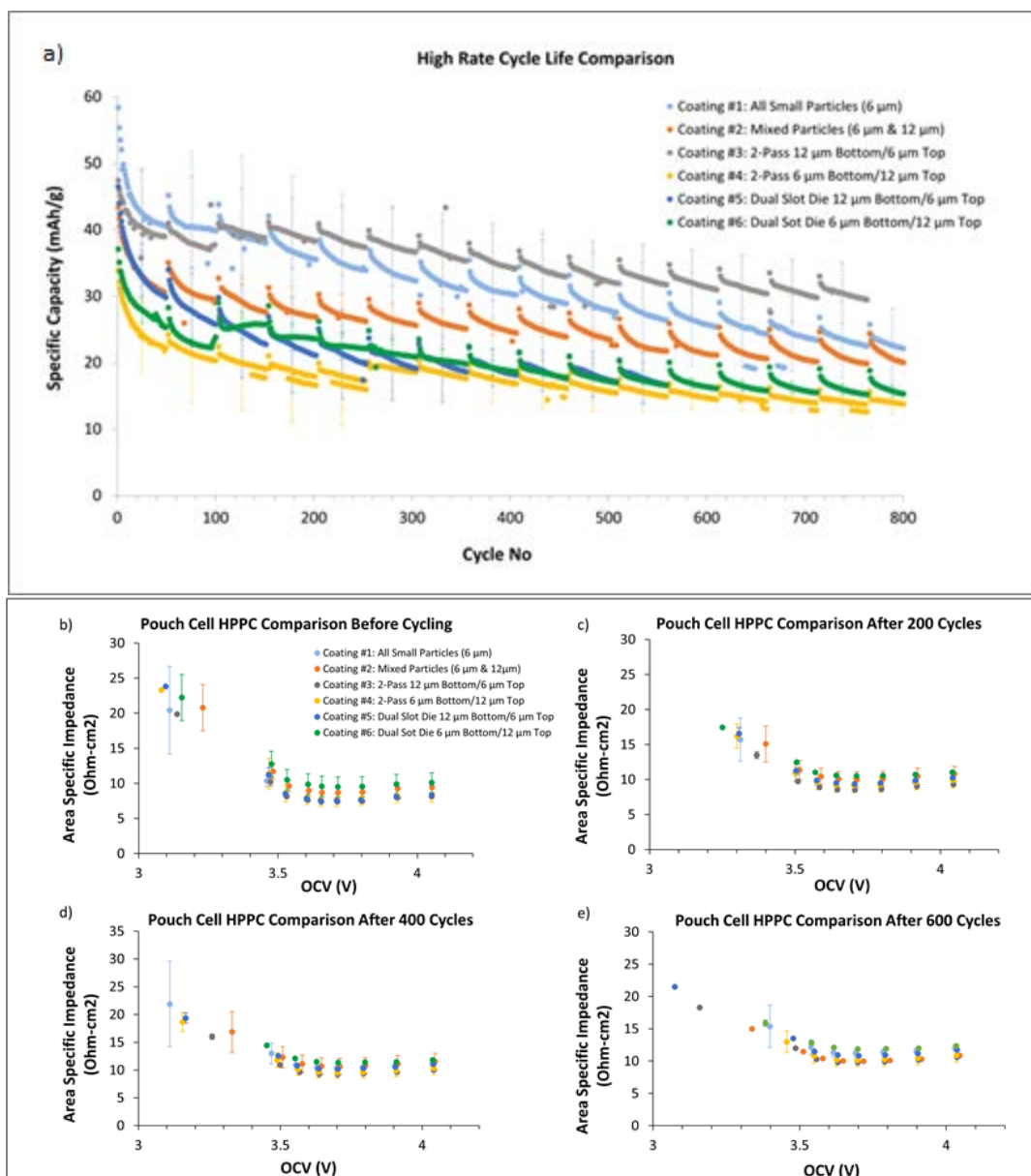


Figure 11. a) First 800 cycles of a high rate pouch cell cycle life study. Charge 1C, Discharge 2C. HPPC was performed every 50 cycles. Each error bar is an average of the standard deviation for those 50 cycles. Data is an average of 2 cells for each coating

(the 3<sup>rd</sup> cell in each coating series has not yet finished enough cycles to include). HPPC results plotted as area specific impedance ( $\text{Ohm}\cdot\text{cm}^2$ ) before cycling (b), after 200 cycles (c), after 400 cycles (d), and after 600 cycles (e). Data points in b – e) without error bars represent only 1 cell.

### Coin Cell Testing Comparison

Figure 12 shows a comparison of the capacity at three different C rates (C/10, C/2, and 2C) for ANL full coin cells, ORNL full coin cells, and ORNL pouch cells made with each coating. The overall trend of the ORNL pouch cells matches the trend observed from the ANL coin cells, showing no significant difference in rate performance between the six coatings. However, while the ORNL pouch cells show slightly higher capacity than the ANL coin cells at lower C rates, the performance of the ORNL pouch cells is substantially lower at 2C (<50% of the capacity of the ANL coin cells). There are a few important differences in the experimental methods that are worth noting. Most significantly, a different electrolyte was used in the two cases (1.2 M  $\text{LiPF}_6$  in 3:7 wt% EC/EMC for the ANL coin cells; 1.2 M  $\text{LiPF}_6$  in 3:7 (v/v) EC/DEC for the ORNL pouch cells).

In addition, the ANL coin cells were made with cathodes calendered to ~40% porosity, while the ORNL pouch cells were made with cathodes calendered to ~35% porosity. Also, the ANL coin cells were cycled between 3.0 and 4.2 V, while the ORNL pouch cells were cycled between 2.5 and 4.2V using a slightly different protocol with a longer formation cycle time and 5 cycles at each C rate (rather than 3).

In order to make a more direct comparison with the ANL coin cells and gain more insight into what may be causing the pouch cell capacity fade at higher C rates, a set of coin cells were made at ORNL using the ANL electrolyte and protocol (but with cathodes calendered to ~35% porosity). The ORNL coin cells showed improved performance at 2C relative to the pouch cells, indicating that the different electrolyte likely makes a difference in the rate performance. However, the capacity at 2C was still quite a bit lower than the ANL coin cells, suggesting that this does not entirely account for the differences (see Figure 12).

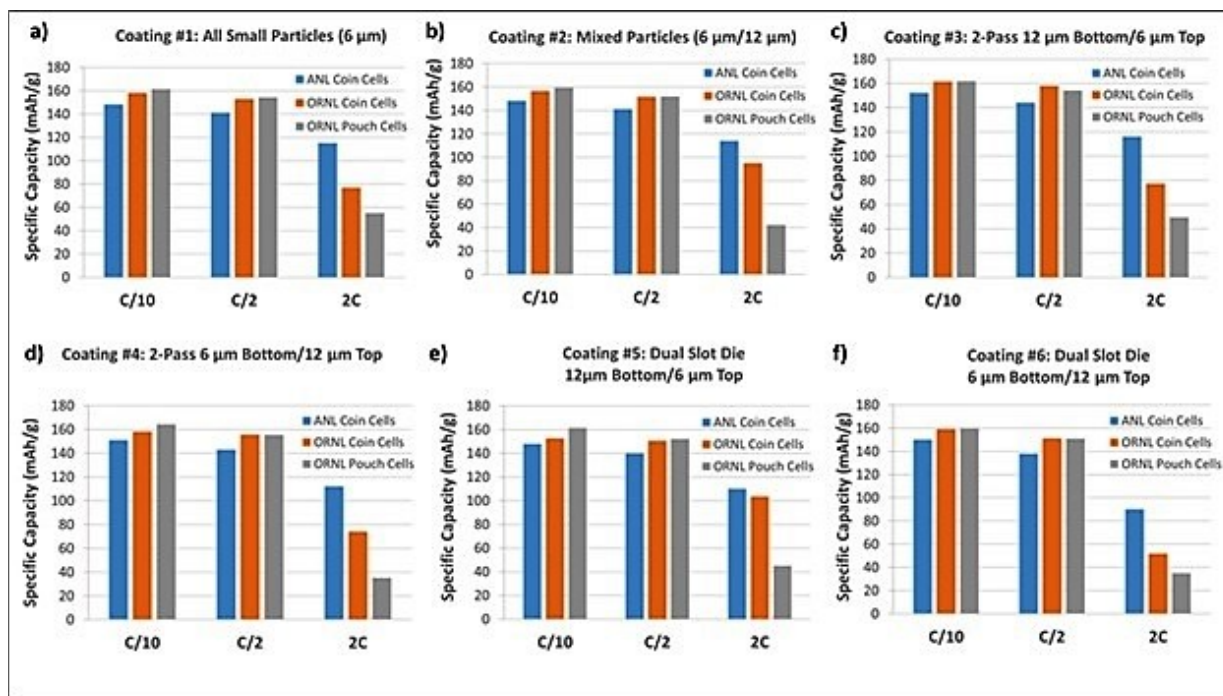


Figure 12. Comparison of capacity at C/10, C/2, and 2C discharge rates for ANL coin cells, ORNL coin cells, and ORNL pouch cells. ANL coin cells data is an average of 4 cells, ORNL coin cell data is an average of 3 cells, and ORNL pouch cell data is an average of 3 cells. a) Coating #1: All Small Particles (6  $\mu\text{m}$ ); b) Coating #2: Mixed Particles (6  $\mu\text{m}$  & 12  $\mu\text{m}$ ); c) Coating #3: 2-Pass

12  $\mu\text{m}$  Bottom/6  $\mu\text{m}$  Top; d) Coating #4: 2-Pass 6  $\mu\text{m}$  Bottom/12  $\mu\text{m}$  Top; e) Coating #5: Dual Slot Die 12  $\mu\text{m}$  Bottom/ 6  $\mu\text{m}$  Top; f) Coating #6: Dual Slot Die 6  $\mu\text{m}$  Bottom/12  $\mu\text{m}$  Top.

### ***Hg Porosimetry Characterization of Cathodes***

Uncalendered (50-55% porosity) and calendered (30% porosity) samples of each coating were sent to Porous Materials, Inc. (PMI) for mercury porosimetry analysis in order to examine possible pore-size distribution (PSD) differences resulting from the different coating architectures. PSDs for both uncalendered and calendered coatings are plotted in Figure 13. The percentage of total pores for each coating in different size ranges is given in Tables VIII and IX.

All six uncalendered coatings have similar PSDs within the lower pore-size mode, with overall pore sizes ranging from  $\sim 90$  nm to 7  $\mu\text{m}$ . However, a few small differences were observed between the coatings. Coating #1 (all small particles, 6  $\mu\text{m}$ ) and Coating 3 (2-Pass, 12  $\mu\text{m}$  bottom/6  $\mu\text{m}$  top) had a slightly higher percentage of pores within the larger mode (between 0.25  $\mu\text{m}$  and 10  $\mu\text{m}$ ) compared to the others, while Coating 6 (Dual slot die, 6  $\mu\text{m}$  bottom/12  $\mu\text{m}$  top) had a slightly higher percentage of the total pores within the smaller mode ( $<0.5$   $\mu\text{m}$ ).

All six calendered coatings had PSDs that were even closer to each other. Interestingly, they all exhibited a third, smaller peak (ranging from  $\sim 3$ -12 nm), which could be a result of creating micropores as the coating is compressed during calendaring, but may also be an artifact from the analysis technique. Again, there are a few small differences between the coatings. Most notably, Coating 1 (all small particles, 6  $\mu\text{m}$ ) had a slightly higher percentage of total pores under 0.01  $\mu\text{m}$  compared to the others, while Coating 5 (Dual slot die, 12  $\mu\text{m}$  bottom/6  $\mu\text{m}$  top) had a slightly higher percentage of larger pores (between 0.25  $\mu\text{m}$  and 10  $\mu\text{m}$ ). However, the overall similarity in PSDs for the six coatings helps explain why there was little observed difference in the rate performance. Also of note is that the bimodal nature of the uncalendered coatings almost disappears after calendaring, further adding to the problem of preserving an advanced electrode architecture during high compression force.

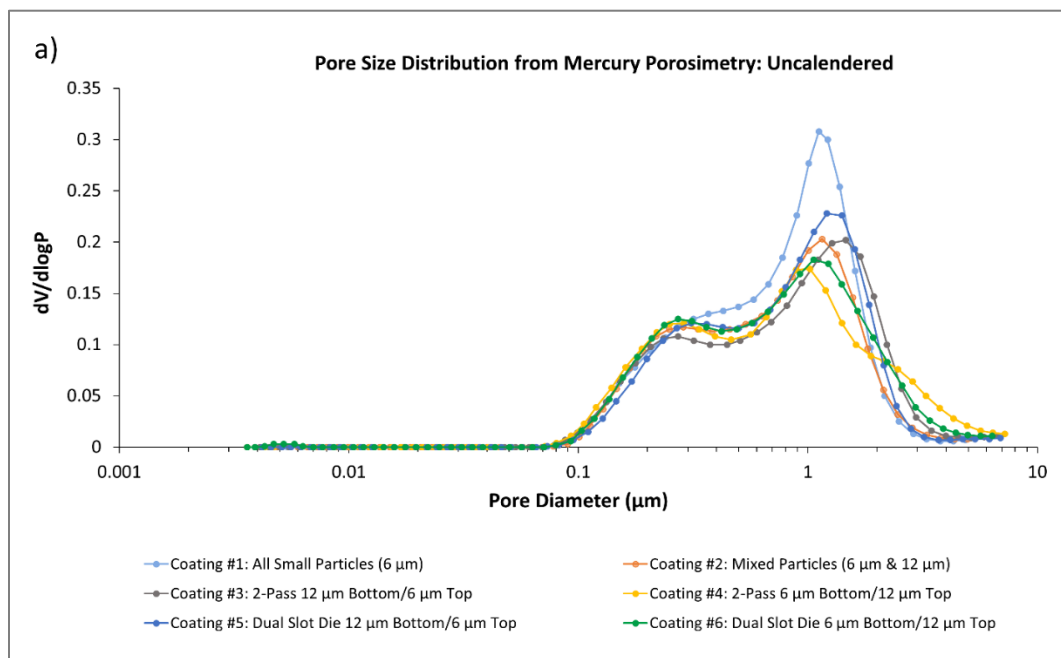


Figure 13a. Pore size distributions calculated from mercury porosimetry measurements of uncalendered (50-55% porosity) coatings.



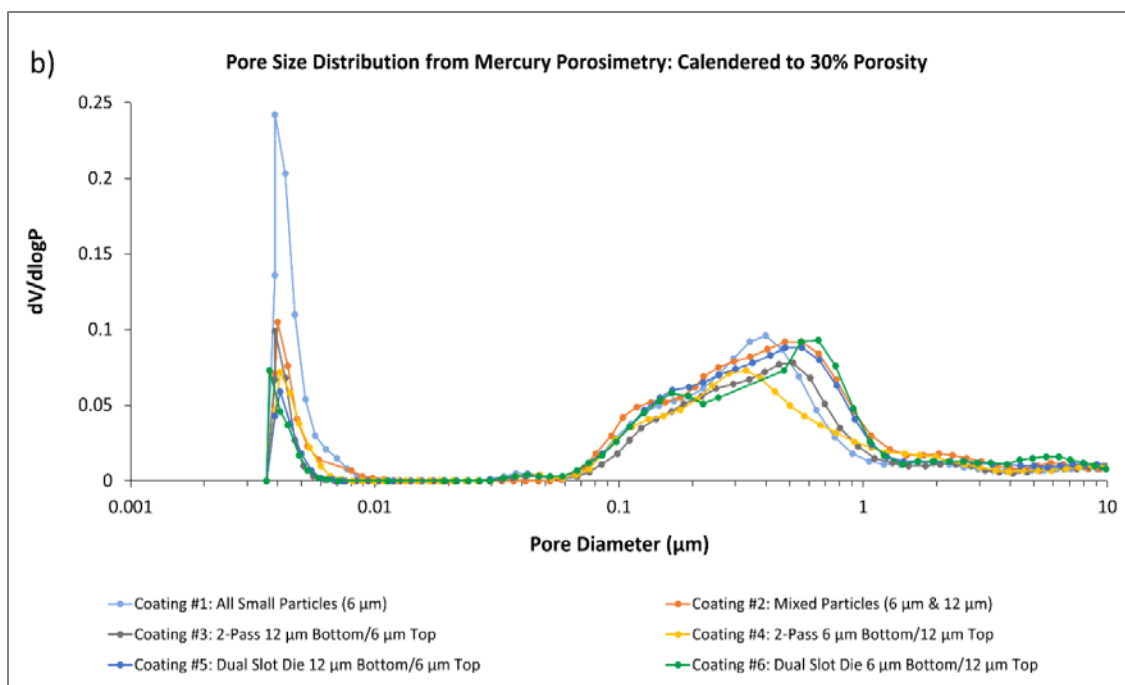


Figure 13b. Pore size distributions calculated from mercury porosimetry measurements of coatings calendered to 30% porosity.

Table VIII. Percentage of total pores in different size ranges calculated from mercury porosimetry analysis of uncalendered (50-55% porosity) coatings.

Coating	% of Pores Under 0.5 $\mu m$	% of Pores Between 0.5 $\mu m$ and 10 $\mu m$
#1 Uncalendered	32	68
#2 Uncalendered	39	61
#3 Uncalendered	32	68
#4 Uncalendered	38	62
#5 Uncalendered	35	65
#6 Uncalendered	40	60

Table IX. Percentage of total pores in different size ranges calculated from mercury porosimetry analysis of coatings calendered to 30% porosity.

Coating	% of Pores Between 0.01 $\mu m$ and 0.25 $\mu m$	% of Pores Between 0.25 $\mu m$ and 10 $\mu m$
#1 Calendered to 30% Porosity	34	66
#2 Calendered to 30% Porosity	32	68
#3 Calendered to 30% Porosity	35	65
#4 Calendered to 30% Porosity	35	65
#5 Calendered to 30% Porosity	31	69
#6 Calendered to 30% Porosity	36	64

## NREL

The first task for NREL was to conduct in-line porosity diagnostics. As-coated electrode samples were received from ORNL in June and July 2016. All samples were spliced into a common roll, the spliced roll was run on the NREL web-line under several test conditions, and porosities were measured. Figure 14 shows the equipment setup for these studies. The raw data was analyzed and shared with the other consortium team members.



Figure 14. NREL web-line with the current porosity NDE configuration and conditions

The measurements did not seem to be sensitive to the distinction between sequentially coated and simultaneously coated (dual slot) layers, as was expected. However, the measurements did appear to be sensitive to the size and arrangement (in layers) of particles in the electrode. This sensitivity is expected to result from differences in thermal properties and/or emissivity due to the different particle sizes and this was predicted by the porosity diagnostic model. A systemic noise source, which was a sub-optimal proportional-integral-derivative (PID) control algorithm, was identified in the porosity measurement setup during runs of the first four samples. This was corrected before continuing testing. Figure 15 illustrates data from second run with all six electrodes at a line speed of 2 ft/min. The results are consistent across all six samples, i.e. small particles on top gives higher response. The origins in the model need further exploration. The results are analogous for dual-pass and dual-slot (simultaneous) samples, i.e. electrodes 4-6 and 3-5, gave very similar results. The systemic noise was greatly reduced to  $\sim 0.1$ . A second run produced the same relative (but lower absolute) responses, at same heat input, at 5 ft/min.

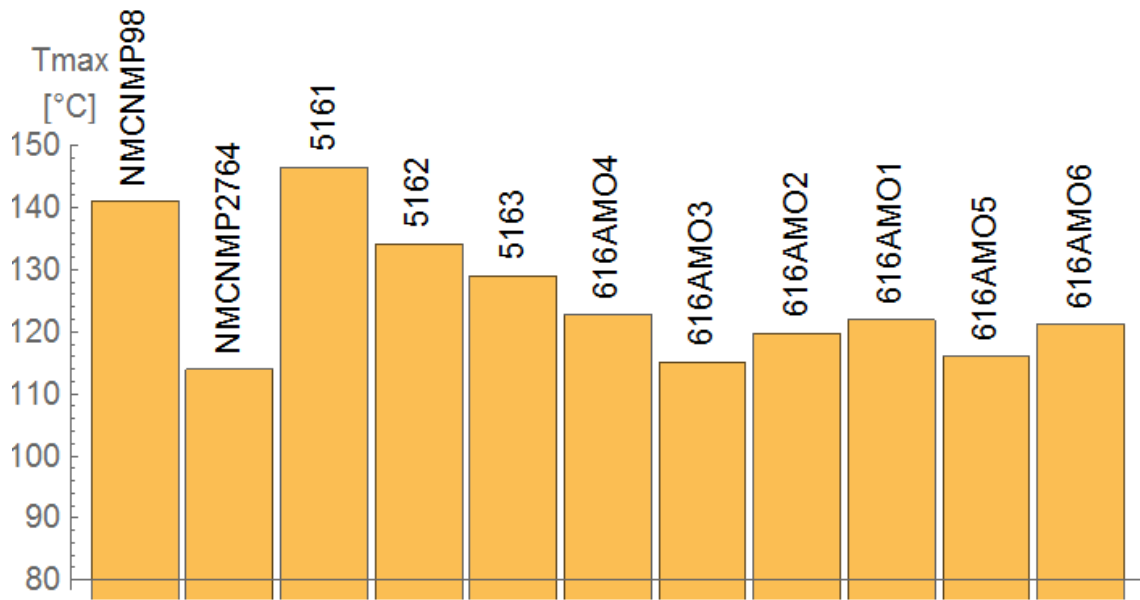
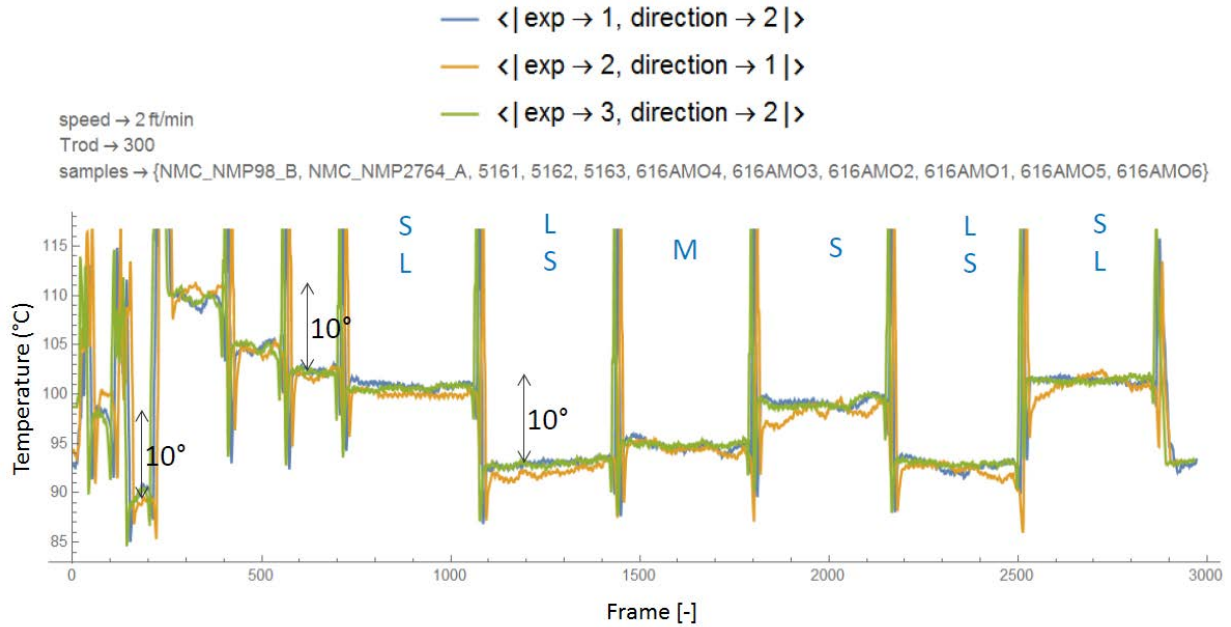


Figure 15. Comparison of NREL porosity (top) and thermal data (bottom) for six electrode samples at 2 ft/min speed

NREL researchers demonstrated the porosity technique on the ORNL coating line with as-coated active layers over a range of coating compositions, thicknesses, and process conditions including at a line speeds up to 10 ft/min. This completed efforts necessary to meet the fourth quarter milestone in the Annual Operating Plan (AOP) for this project. The research focused solely on cathodes, as this is the more critical layer relative to cost and performance in the battery structure. Also, both active and passive thermography techniques were evaluated. NREL will down-select active thermography methods for the purpose of determining directions for further development of the porosity technique. However, passive thermography may still be assessed in the future for discrete defect detection or other desired measurements. These materials made using R2R will be highly useful in the ongoing validation of the technique under the consortium.

The second task for NREL was to install and start operating the XRF for electrode characterization. This required working with the XRF device developer (XOS<sup>®</sup>), sensor manufacturer (Amptek) and system

integrator (PMD Inc.) to obtain design and operational information as necessary to re-commission the system. A local controls engineering firm (Mountain Peak Controls) was contracted to successfully de-integrate the operation and data acquisition aspects of the XRF system from the original in-line controls and configuration setup. After this, NREL completed construction of the XRF mounting stand, including a safety guard, interlocks, and sample handling. The system was commissioned with state certification and a NREL Environmental Health and Safety Readiness Verification and Safe Work Permit. The XRF system as shown in Figure 16 is fully operational and will be used for future R2R efforts.



Figure 16. XRF setup at NREL

The XRF was used to complete measurements of the first replicate of 11 different cathode samples, including the six from this project as well as five from a VTO-funded collaboration with ORNL. The latter samples were selected and included to broaden the range of loading and composition in our sample set. Data from this first replicate set was analyzed using a new software that facilitates signal analysis and atom-specific corrections. Results for these analyses are shown in Figure 17. A second and third replicate set will also be measured for statistical purposes.

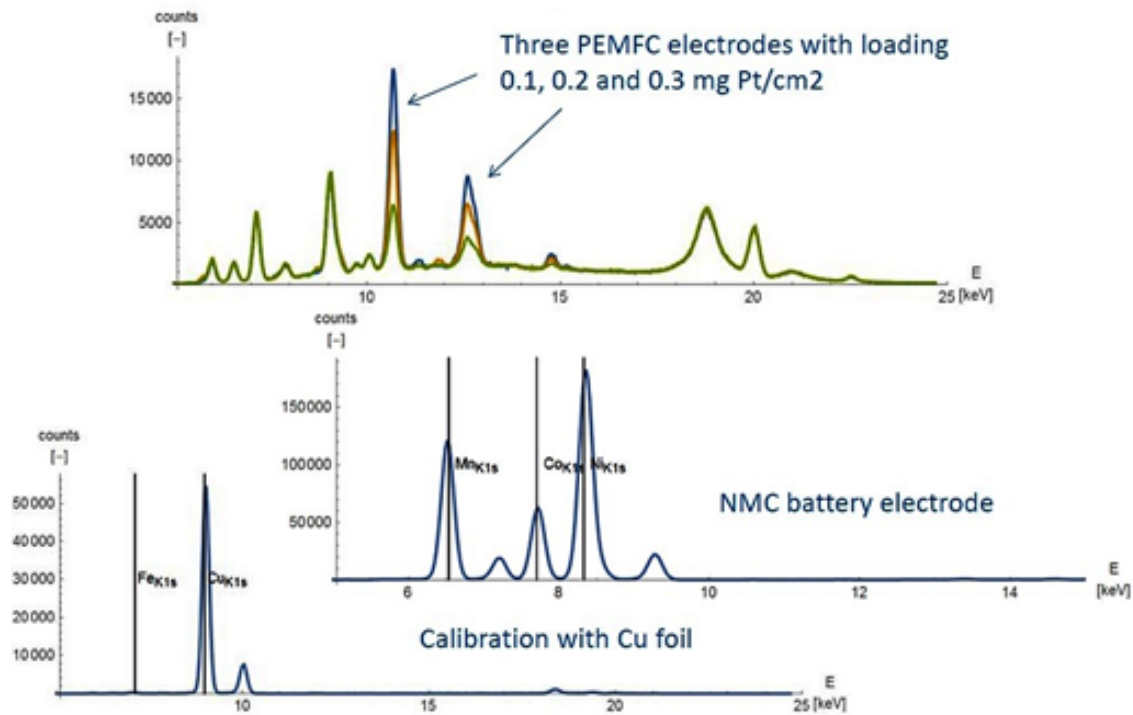


Figure 17. XRF analysis of PEMFC and NMC electrodes

The last NREL task was to modify an existing porosity diagnostic model to include a two or more layer construction of electrodes. This was completed during the fourth quarter of FY 2016. Using this model, NREL determined that the materials differences (different particle sizes) alone would not have caused the difference in measured thermal response that was observed in the six coated cathode samples from ORNL (see Figure 15 above). The SEM imaging from ANL clearly shows significant differences in surface structure between the electrodes with small particles in the top layer, and those with large particles in the top layer, which is consistent with results obtained from the model. This could result in a change in surface reflectance and emissivity between samples. NREL modified these properties and conditions in the model using sensible estimates, and found that differences in emissivity and reflectance in the different cathode samples, based on their surface structure, could definitely result in the differences in measured thermal response that were observed.

## LBNL

The objective of the LBNL effort was to develop predictive capabilities for manufacturing processes, connecting process variables to product performance, with initial focus on understanding the fabrication process of porous composite battery electrodes. This required personnel with vast experience in predicting material synthesis conditions, high performance computing of processing, and visualization of processing and performance modeling. In addition, facilities for conducting the slurry drying experiments required that a ventilation system for working with NMP-based slurries at the beamline had to be designed and built. A system to accurately dispense small volumes (microliters) of high-viscosity slurries was designed for the droplet experiments. Data processing tools to reduce the influence of imaging artifacts required development. The process LBNL used to develop predictive capabilities for the electrode materials is depicted in Figure 18.



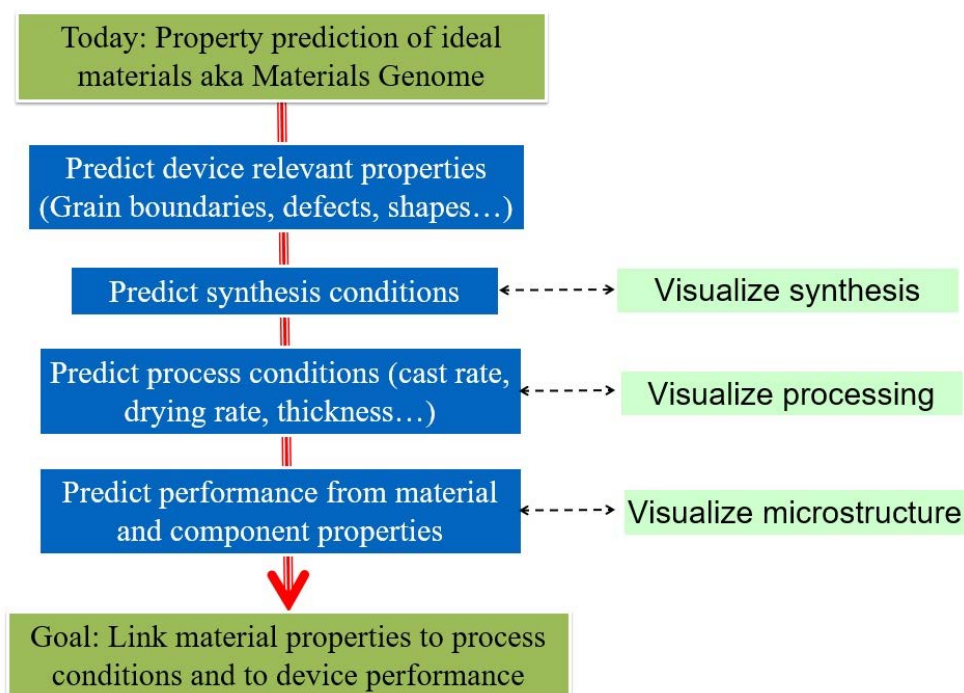


Figure 18. LBNL process flow for a predictive capability to accelerate materials adoption

X-ray radiography and tomography were used to capture the evolution of the NMC particles in a slurry to the formation of the electrode. X-ray radiography was performed at frequent intervals (e.g. 15 sec). Tomography was performed on electrode samples with images taken from many angles that required longer acquisition times, which was not suitable for a dynamic system. These studies were the first to report two-dimensional and three-dimensional visualization of battery electrode drying. Figure 19 illustrates a computer simulation and visualization of one of the electrode materials received from ORNL (image rotates to the right).

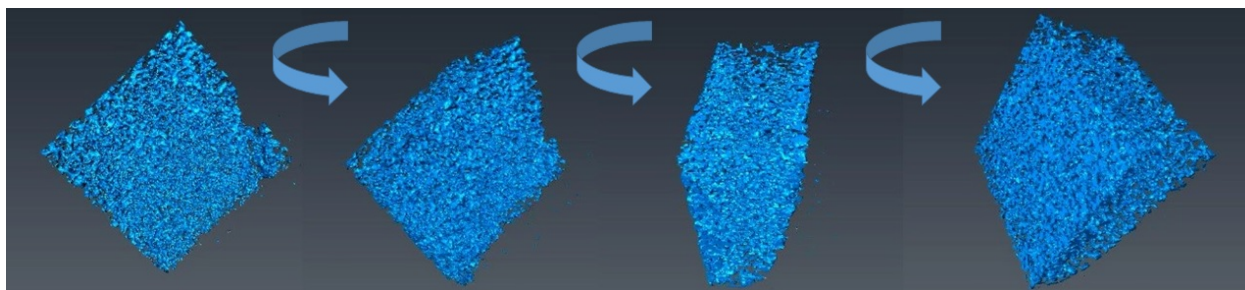


Figure 19. Computer three-dimensional visualization of battery electrode material with NMC particles

To conduct the droplet studies, a modified set-up for commercial slurries was used as shown in Figure 20. Slurries were made using 6 $\mu$ m and 12 $\mu$ m NMC and carbon black (CB) particles in PVDF/NMP. The composition of the slurry was 55 wt% NMP, 20.5 wt% NMC, 2.25 wt% PVDF, and 2.25 wt% CB. The slurry preparation procedure was conducted in a glove box by adding PVDF to NMP, homogenizing for 10min @ 1200rpm, adding NMC, homogenizing for 20min @ 1200rpm, and adding CB, homogenize for 10min @ 1200rpm. The slurry was then loaded into a syringe and attached to a customized syringe driver. The drop volume was precisely controlled by a micrometer. Figure 20 shows schematically the experimental setup for conducting the radiography experiments of drying a droplet.

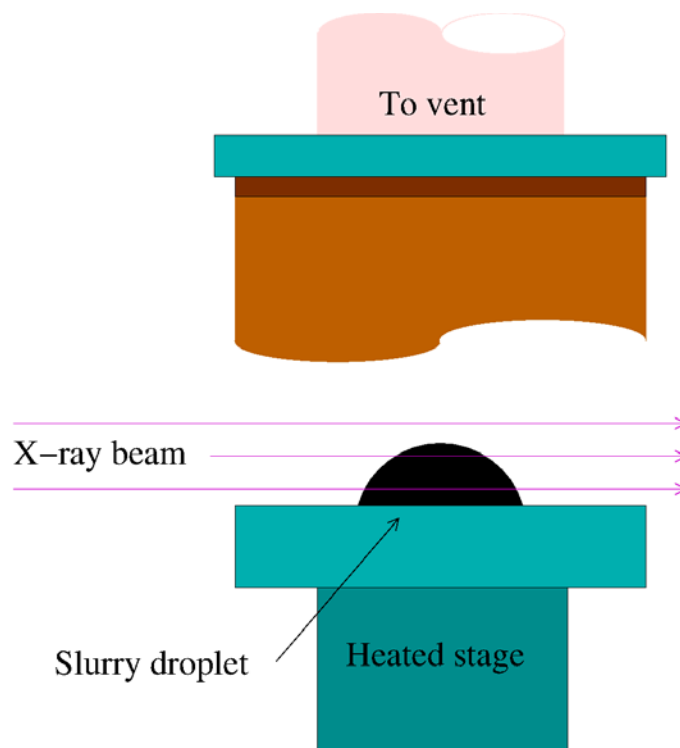


Figure 20. Experimental setup for radiography of drying drop.

Studies with dilute vs. viscous slurries showed clear differences between SiO in water and NMC, 6 $\mu$ m particles in NMP at 60°C for 20 mins. When a mixed particle laminate sample was analyzed, the porosity was calculated starting at the bottom of the sample going to the top using tomography. With certain shapes, there are artifacts depending on the angle of the x-ray beam to the sample. For example, the approximate porosity for a laminate and the dried droplet model are the same for the first 50 $\mu$  of thickness but then, due to the artifacts of rotating the sample in the beam, the porosity of the dried droplet increases as you get near the surface. So the shape of the sample needs to be fixed. Tomography images showed that the viscosity clearly changes dynamics from a coffee ring to a frozen configuration. The viscous slurry showed similar thickness changes to R2R processed materials so this technique can be used to study process conditions. Figure 21 shows images and results for the study of an electrode material formed in the droplet studies versus the laminate electrode material received from ORNL made with a R2R process. The model system shows similar behavior to the real R2R laminates within the first 50 $\mu$ m of the laminate. Figure 22 shows the simulated discharge curves for cell potential vs. capacity at two rates for half-cell with the NMC electrode. The highest capacity was achieved at 1C rate for the 6 $\mu$ m particle size.



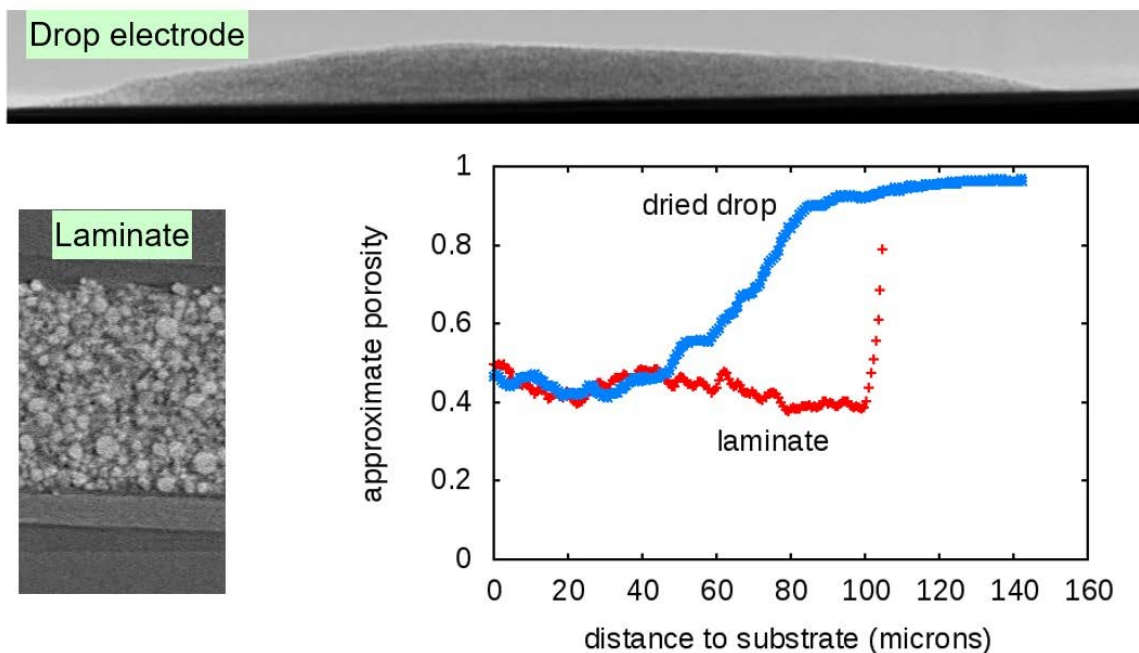


Figure 21. Comparison of a droplet formed electrode material vs a R2R laminate electrode material (Top: Radiography image of drying NMC/CB/PVDF/NMP drop showing particle settling)

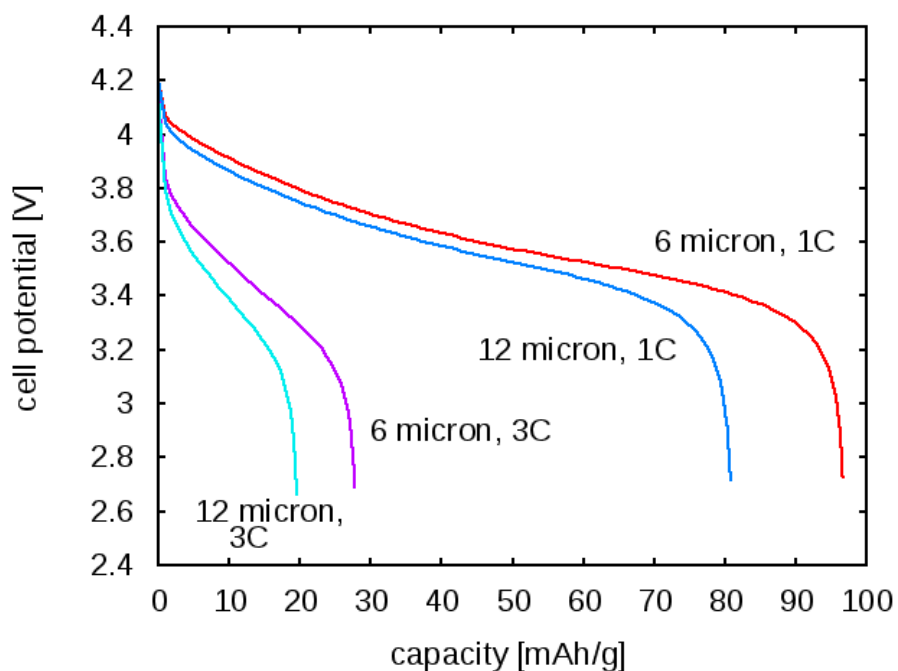


Figure 22. Simulated discharge curves at two rates for half-cell with NMC electrode.

For the particle settling model, LBNL implemented particle-particle and particle-wall interactions for a slurry drop packed with spherical particles. This included background fluid forces, both isotropic and rotational. A thin fluid film was maintained between spheres as a repulsive force to keep spheres from touching. Extensive testing was performed to verify that this is physically accurate. The particle settling model uses an algorithm

based on adaptive finite volume methods in the Chombo software framework which supports high performance computing. LBNL started by looking at 3000 particles and reduced this to just a few to be able to do direct mechanical simulation where every particle is part of the computation domain. The particle-to-particle interaction that looks at particles merging was assessed and artificial forces are created to repel them. When the viscous slurries were examined, there was a hydrodynamic effect when two particles come together and the increase in velocity makes them want to agglomerate, which hasn't been observed yet but still needs to be included in the mathematical calculations to be as realistic as possible. COMPRO software was used to do adaptable meshing, so when there are particles falling down there is a lot more meshes near the particle-liquid interface and when a real time calculation is needed. Another approach was to "push down" on particles to see how much they can be packed.

When particle dynamics are being modeled in a settling process, some particles move up and some move down. To understand why this happens, LBNL looked at the velocity fields. A cluster of larger particles tends to settle downward due to gravity. The liquid displaces some of the particles and moves to a region where there are less particles. When the velocity of the liquid goes upward, the particles go up with the liquid.

### **Collaboration/Coordination/Outreach**

The built-in consortium-based collaboration only recently started but the labs collaborated well, sharing materials, data and techniques. ANL supplied cathode powders to ORNL and ORNL supplying cathode electrode coatings to the other three partner labs. ANL involved Citrine to examine a wide range of pertinent electrochemical testing, characterization performance and life data to determine which adjustable parameters most strongly influence performance and life of the electrode coating materials. ORNL and NREL routinely discussed details related to accelerating the timeline for having in-line XRF operational at NREL. NREL participated in project calls, participated in project meetings at AMR and Kodak, coordinated with ORNL on configuration and receipt of electrode sheet samples, and generically discussed project with industry partners to gauge their interest to participate. LBNL analyzed and generated models of laminate samples and NMC particles received from ORNL and ANL. Specific consortium efforts for each laboratory were as follows:

#### **ANL**

- Supplied NMC particles to ORNL for R2R manufacture of electrode materials.
- Provided battery electrode research data to ORNL and Citrine for further analysis.
- Collaborated with Citrine during the development of a machine learning model for improving cathode design.

#### **ORNL**

- Supplied cathode electrode coatings to the other three partner labs for testing.
- Received cathode powders from ANL to form cathode materials.
- Received baseline anode coatings for extensive pouch cell builds with cathode Coatings 1-6
- Exchanged detailed coin cell performance data obtained with the six different cathodes with ANL.
- Discussed details that led to the acceleration of the timeline for having in-line XRF operational and the in-line porosity measurement method in place with active infrared (IR) thermography with NREL.
- Participated significantly in biweekly project calls and the onsite review meetings at Eastman Kodak and ORNL, as well as made meaningful contributions to the FY 2017 joint ORNL/NREL AOP.
- Continued Consortium discussions with industry partners in anticipation of an industry CRADA solicitation.
- Addressed the third quarter milestone for ORNL/NREL by having multiple discussions with battery manufacturers such as XALT<sup>®</sup> Energy, Navitas Systems, and Kodak on R2R NDE and enhanced QC

for electrode production. These discussions focused on in-line IR thermography, XRF, and low-cost thickness measurement.

## **NREL**

- Participated in consortium efforts with partner labs and at team and project review meetings with the AMO Program Manager.
- Provided Strength, Weaknesses, Opportunities and Threats (SWOT) analysis in collaboration with Eastman Kodak Business Park for other applications of R2R such as fuel cells and electrolyzers.
- Coordinated with consortium partners to provide inputs to the FY2017 project proposal and AOP.
- Coordinated with ORNL on details of XRF analysis and next steps for a porosity technique.
- Continued to discuss the consortium with industry partners in anticipation of an industry solicitation.
- Addressed third quarter milestone for input on quality control (QC) from three industry partners. Examples are communications with fuel cell companies over the last six months, to determine the needs for in-line membrane thickness measurement, especially if it could provide real-time mapping; in-line measurement of membrane defects, especially including identification and classification of foreign particles; in-line detection of delamination of multi-layer constructions; detection of defects leading to shorting and/or hydrogen crossover in an MEA; and better understanding of the performance and lifetime effects of several different kinds of defects in MEAs.

## **LBNL**

Utilized laminate samples and NMC particles from ORNL and ANL for the experimental modeling efforts.

- Compared mercury porosimetry data from ORNL to LBNL experimental modeling results.

## **Challenges/Contingencies**

The ANL effort was on an accelerated schedule to achieve results in a shortened amount of time. Commercial materials were utilized which enabled a faster turnaround. When custom materials are needed, it will take longer and more effort to provide the materials and electrode coatings.

For NREL, challenges were in getting the XRF system, which was designed and integrated for a different application, safely operational to ensure that the porosity measurement system had appropriate sensitivity for new electrode structures. NREL and ORNL will determine a specific measurement approach with the XRF system to ascertain if it can be more accurate/useful in measuring cathode active material loadings than was previously seen by ORNL. They will also identify high-impact pathways for future consortium activities.

ORNL utilized the commercially-available active materials supplied by ANL for fabricating the electrodes because of time constraints in getting custom materials. Performance results for the cathodes made with these materials were expected to be better than other materials currently being used by manufacturers.

For LBNL efforts, available beamtime is always a limited resource and can strongly influence the schedule under which tasks are completed. LBNL was able to schedule beamtime to meet the project milestones for FY 2016. The refinement of particle suspension model will involve two main challenges: (1) proper handling of N sphere interactions and (2) determination of appropriate boundary conditions for sphere interactions near the boundary of the domain. The dried NMC/CB/PVDF/NMP droplets used in the LBNL experiments were found to be asymmetric, limiting qualitative image analysis and subsequent comparison of porosity gradients with the ORNL electrodes. In addition, the dried drops were highly non-uniform in thickness, complicating meaningful comparison with the electrodes. An effort on preliminary dynamic slurry simulation should focus on fully-developing the hydrodynamic component to produce a high-quality particle settling simulation before adding a drying model. The current particle settling simulation provides a foundation for a slurry drying simulation.

## **Risks and Risk Handling**

### **ANL**

Risk: Custom materials are needed to enhance performance which take longer to produce and provide the materials for electrode coatings.

Mitigation: Commercial materials (NCM 523 particles) were used to enable a faster turnaround for making the electrode coatings.

Risk: The Citrine data model may not be able to analyze material synthesis process data and cell performance data to determine synthesis conditions for optimizing material chemical and electrochemical performance with the available data.

Mitigation: ANL will work closely with Citrine and provide any additional data that may be able to be collected during the large scale material synthesis.

### **ORNL**

Risk: Additional time may be needed to collect sufficient USABC durability data (0.33C/-0.33C) on Coatings 1-6 at the full pouch cell scale.

Mitigation: ORNL will conduct accelerated durability testing at 1C/2C to obtain high-rate capacity fade, which holds more relevance to the cathode Coatings 1-6 designs.

Risk: Cathode Coatings 1-6 did not show distinct and fully conclusive performance differences.

Mitigation: The plan for FY 2017 is to redesign the cathode architectures, perhaps with and without calendaring, and add an advanced anode coating matrix to the electrode production, coin cell testing, and pouch cell testing plans.

### **NREL**

Risk: The electrode porosity NDE technique will not be sensitive to changes in the new electrode structures.

Mitigation: Provide technique design improvements – such as increasing the thermal output of the radiative heat source – and a wide range of operating conditions to ensure sufficient sensitivity. This risk was mitigated in the fourth quarter of FY 2016.

Risk: XRF system accuracy and sensitivity for new electrode structures is not sufficient for real-time porosity measurement of cathode active material loading.

Mitigation: In coordination with ORNL, NREL established a measurement protocol to maximize the probability of getting sufficient accuracy ensuring that the porosity measurement system has appropriate sensitivity for new electrode structures, and identifying high-impact pathways for future consortium activities.

Risk: The porosity model will not sufficiently represent the new electrode structures.

Mitigation: To date, analyses with the updated model have predicted the observed thermal responses. Actual physical measurements of emissivity and thermal conductivity of the cathode layers were made to further augment the model.

## **LBNL**

**Risk:** Based on preliminary slurry drying experiments, as well as earlier experience with NMC electrodes, there should be no risks in the x-ray imaging process. However, future work will involve more viscous slurries, so dispensing uniform droplets will be more difficult than in the preliminary experiments.

**Mitigation:** While this risk is low due to mitigation through designing a droplet dispensing system with these challenges in mind, the system is still under construction and is therefore untested. Testing will be performed before any scheduled beamtime. Poor performance will cause the droplet images to be difficult to analyze, so the risk will be mitigated by exploring alternative approaches to dispensing the slurry.

**Risk:** Beamtime is never guaranteed, and unscheduled downtime is always a possibility.

**Mitigation:** Beamtime has been managed effectively at the LBNL Advanced Light Source so the probability of risk is low. Delays in securing beamtime could introduce delays into the experimental schedule. Another approach for future experimentation is to apply for beamtime at other x-ray sources. This will mitigate risk and may make additional techniques available for future project directions. Beamtime for experiments in FY 2016 was secured to complete analysis of all electrode materials.

**Risk:** Personnel in the Energy Storage Group is leaving LBNL

**Mitigation:** A new LBNL Lab Team Lead has been assigned to this project for future funded efforts on this project.

## Technology Transfer Path

The R2R AMM DOE Laboratory Consortium will execute the program with industry through a partnership with Kodak Eastman Business Park and with a CRADA data call to enable manufacturers to realize the R2R potential for manufacturing commercial products. Kodak Eastman Business Park has an extensive suite of tools to assist small companies including a key set of development apparatus to conduct early and mid-stage pilot work. They can also provide technical resources to industry clients in a manner that is protective of intellectual property to assist in bringing immature technologies to the commercial market – from scale up to full production. This DOE-Industry partnership will result in low manufacturing costs, low energy processes, high volume production, high throughput due to thinner materials, compatibility with many material platforms, and products with varying sizes and dimensions.

The CRADA effort will have a 10 to 18-month execution that will result in an increase in the MRL level for a given technology because all proposed barriers to technology transfer will be removed. This will allow technology alignment with EERE and consortium goals using the application of primary metrics of success, i.e., throughput, energy, and yield.

## Conclusions

The R2R AMM DOE Laboratory Consortium successfully completed all tasks on an accelerated schedule to develop a materials synthesis process using a R2R manufacturing process and to provide modeling, simulation, processing, and manufacturing techniques that demonstrate the feasibility of the scale-up potential for enhanced battery electrodes. The research efforts predicted and measured changes and results in electrode morphology and performance based on process condition changes. The consortium team evaluated mixed, active, particle size deposition and drying for novel electrode materials and assessed various process changes and the resulting morphology and electrode performance. Specific conclusions for each of the labs are as follows:

ANL conducted a significant amount of work in a short amount of time. As seen in the data, some of the cathode architectures are performing better than others. From the data the Double Pass 12B $\mu$ :6 $\mu$ T is the best performing cells so far, but close behind are the 6 $\mu$ m only cells and the Single Pass 6 $\mu$ B:12T cells. The other cells show a lower capacity retention and are grouped together. The Double Pass 6B:12 $\mu$ T cells and the 6 $\mu$  and 12 $\mu$  Blended cells are about the same and the Single Pass 12 $\mu$ B:6 $\mu$ T is lowest performing so far. With this data, there are no specific trends on what cathode architecture works the best. Further testing and analysis is needed to fully understand the cathode architecture and how to design the electrode that will take advantage of the electrode structure.

ORNL completed all coatings by the end of the third quarter of FY 2016 and performance testing was ~75% completed prior to the end of FY 2016. The primary conclusion is that calendering of the advanced cathode designs homogenized all six coatings into structures with similar PSDs and almost completely eliminated the bimodal structure that was part of the PSD gradient. The calendering may have also reduced the total porosity of the six electrode architectures too much to see significant differences between them.

NREL modified an existing porosity diagnostic model to include two or more layers of construction for electrodes. The SEM imaging from ANL clearly shows significant differences in surface structure between the electrodes with small particles in the top layer, and those with large particles in the top layer, which is consistent with results obtained from the model. This could result in a change in surface reflectance and emissivity between samples. These properties and conditions were modified in the model using sensible estimates, and found that differences in emissivity and reflectance in the different cathode samples, based on their surface structure, could definitely result in the differences in measured thermal response that were observed.

LBNL developed and demonstrated experimental and modeling capabilities for electrodes, providing a framework for further research in the area of porous electrode fabrication. All milestones were met, with the exception of drop/coating comparisons that could not be done meaningfully in light of experimental observations, as well as of reallocation of efforts toward hydrodynamic interactions of particles rather than on evaporation in suspension simulations. LBNL developed the first steps to predict synthesis conditions and a capability to visualize processing. The current model system represents reality and is the first steps toward developing process models.



## Glossary

1C, 2C, C/3, C/5, C/10, C/20	Charge and discharge rates of a battery are governed by C-rates. The capacity of a battery is commonly rated at 1C, meaning that a fully charged battery rated at 1Ah should provide 1A for one hour. The same battery discharging at 0.5C should provide 500mA for two hours, and at 2C it delivers 2A for 30 minutes. Losses at fast discharges reduce the discharge time and these losses also affect charge times. [2]
Brunauer, Emmett, Teller	Brunauer–Emmett–Teller (BET) theory aims to explain the physical adsorption of gas molecules on a solid surface and serves as the basis for an important analysis technique for the measurement of the specific surface area of a material. [3]
Calendering	A finishing process used on cloth, paper, or plastic film. A calender is employed, usually to smooth, coat, or thin a material. [4]
Coin cell	A single-cell battery that is used to power wristwatches, computer clocks, hearing aids and other small devices. Also called a "coin cell," button cells look like small, squat silver cans from five to 25mm in diameter. [5]
Dual slot	A process that allows splitting of the required amount of material into two layers and then applying them simultaneously on a substrate.
Hybrid Pulse Power Characterization (HPPC)	Test procedure whose results are used to calculate pulse power and energy capability under specific operating conditions. [6]
Manufacturing Readiness Level	A measure developed by the United States Department of Defense (DOD) to assess the maturity of manufacturing readiness, similar to how Technology Readiness Levels (TRL) are used for technology readiness. Table X provides definitions for the various levels of MRLs. Figure 23 illustrates the relationship of MRL to TRLs for systems acquisitions. [7]

Table X. Material Readiness Level Definitions [7]

## Manufacturing Readiness Levels

Relative Level of Manufacturing Development	Manufacturing Readiness Level	MRL Definition	Description
Full rate production demonstrated and lean production practices in place	<b>MRL 10</b>	This is the highest level of production readiness. Technologies should have matured to TRL 9	This level of manufacturing is normally associated with the Production or Sustainment phases of the acquisition life cycle. Engineering/design changes are few and generally limited to quality and cost improvements. System, components or items are in full rate production and meet all engineering, performance, quality and reliability requirements. Manufacturing process capability is at the appropriate quality level. All materials, tooling, inspection and test equipment, facilities and manpower are in place and have met full rate production requirements. Rate production unit costs meet goals, and funding is sufficient for production at required rates. Lean practices are well established and continuous process improvements are ongoing. Although the MRLs are numbered, the numbers themselves are unimportant. The numbers represent a non-linear ordinal scale that identifies what maturity should be as a function of where a program is in the acquisition life cycle. Using numbers is simply a convenient naming convention.
Manufacturing concepts identified; low rate production demonstrated; capability in place to begin full rate production	<b>MRL 9</b>	The system, component or item has been previously produced, is in production, or has successfully achieved low rate initial production.	Technologies should have matured to TRL 9. This level of readiness is normally associated with readiness for entry into Full Rate Production (FRP). All systems engineering/design requirements should have been met such that there are minimal system changes. Major system design features are stable and have been proven in test and evaluation. Materials, parts, manpower, tooling, test equipment and facilities are available to meet planned rate production schedules. Manufacturing process capability in a low rate production environment is at an appropriate quality level to meet design key characteristic tolerances. Production risk monitoring is ongoing. LRIP cost targets have been met, and learning curves have been analyzed with actual data. The cost model has been developed for FRP environment and reflects the impact of continuous improvement.
Pilot line capability demonstrated; ready to begin Low Rate Initial Production (LRIP)	<b>MRL 8</b>	Associated with readiness for a Milestone C decision, and entry into Low Rate Initial Production (LRIP).	Technologies should have matured to at least TRL 7. Detailed system design is complete and sufficiently stable to enter low rate production. All materials, manpower, tooling, test equipment and facilities are proven on pilot line and are available to meet the planned low rate production schedule. Manufacturing and quality processes and procedures have been proven in a pilot line environment and are under control and ready for low rate production. Known producibility risks pose no significant challenges for low rate production. Cost model and yield and rate analyses have been updated with pilot line results. Supplier qualification testing and first article inspection have been completed. The Industrial Capabilities Assessment for Milestone C has been completed and shows that the supply chain is established to support LRIP.
Capability to produce systems, subsystems, or components in a production representative environment	<b>MRL 7</b>	Typical for the mid-point of the Engineering and Manufacturing Development (EMD) Phase leading to the Post-CDR Assessment. Technologies should be on a path to achieve TRL 7.	System detailed design activity is nearing completion. Material specifications have been approved and materials are available to meet the planned pilot line build schedule. Manufacturing processes and procedures have been demonstrated in a production representative environment. Detailed producibility trade studies are completed and producibility enhancements and risk assessments are underway. The cost model has been updated with detailed designs, rolled up to system level, and tracked against allocated targets. Unit cost reduction efforts have been prioritized and are underway. Yield and rate analyses have been updated with production representative data. The supply chain and supplier quality assurance have been assessed and long-lead procurement plans are in place. Manufacturing plans and quality targets have been developed. Production tooling and test equipment design and development have been initiated.
Capability to produce a prototype system or subsystem in a production relevant environment	<b>MRL 6</b>	Associated with readiness for a Milestone B decision to initiate an acquisition program by entering into the Engineering and Manufacturing Development (EMD) Phase of acquisition.	Technologies should have matured to at least TRL 6. It is normally seen as the level of manufacturing readiness that denotes acceptance of a preliminary system design. An initial manufacturing approach has been developed. The majority of manufacturing processes have been defined and characterized, but there are still significant engineering and/or design changes in the system itself. However, preliminary design has been completed and producibility assessments and trade studies of key technologies and components are complete. Prototype manufacturing processes and technologies, materials, tooling and test equipment, as well as personnel skills have been demonstrated on systems and/or subsystems in a 2-4 production relevant environment. Cost, yield and rate analyses have

			been performed to assess how prototype data compare to target objectives, and the program has in place appropriate risk reduction to achieve cost requirements or establish a new baseline. This analysis should include design trades. Producibility considerations have shaped system development plans. The Industrial Capabilities Assessment (ICA) for Milestone B has been completed. Long-lead and key supply chain elements have been identified.
Capability to produce prototype components in a production relevant environment	MRL 5	Typical of the mid-point in the Technology Development Phase of acquisition, or in the case of key technologies, near the mid-point of an Advanced Technology Demonstration (ATD) project.	Technologies should have matured to at least TRL 5. The industrial base has been assessed to identify potential manufacturing sources. A manufacturing strategy has been refined and integrated with the risk management plan. Identification of enabling/critical technologies and components is complete. Prototype materials, tooling and test equipment, as well as personnel skills have been demonstrated on components in a production relevant environment, but many manufacturing processes and procedures are still in development. Manufacturing technology development efforts have been initiated or are ongoing. Producibility assessments of key technologies and components are ongoing. A cost model has been constructed to assess projected manufacturing cost.
Capability to produce the technology in a laboratory environment	MRL 4	Acts as an exit criterion for the Materiel Solution Analysis (MSA) Phase approaching a Milestone A decision.	Technologies should have matured to at least TRL 4. This level indicates that the technologies are ready for the Technology Development Phase of acquisition. At this point, required investments, such as manufacturing technology development, have been identified. Processes to ensure manufacturability, producibility, and quality are in place and are sufficient to produce technology demonstrators. Manufacturing risks have been identified for building prototypes and mitigation plans are in place. Target cost objectives have been established and manufacturing cost drivers have been identified. Producibility assessments of design concepts have been completed. Key design performance parameters have been identified as well as any special tooling, facilities, material handling and skills required.
Manufacturing proof of concept developed	MRL 3	Validation of the manufacturing concepts begin through analytical or laboratory experiments	This level of readiness is typical of technologies in Applied Research and Advanced Development. Materials and/or processes have been characterized for manufacturability and availability but further evaluation and demonstration is required. Experimental hardware models have been developed in a laboratory environment that may possess limited functionality.
Manufacturing concepts identified	MRL 2	Characterized by describing the application of new manufacturing concepts	Applied research translates basic research into solutions for broadly defined military needs. Typically this level of readiness includes identification, paper studies and analysis of material and process approaches. An understanding of manufacturing feasibility and risk is emerging.
Basic manufacturing implications identified	MRL 1	Lowest level of manufacturing readiness	The focus is to address manufacturing shortfalls and opportunities needed to achieve program objectives. Basic research (i.e., funded by budget activity) begins in the form of studies.

Source: Manufacturing Readiness Level (MRL) Deskbook Version 2.0, Prepared by the OSD Manufacturing Technology Program in collaboration with The Joint Service/Industry MRL Working Group, May, 2011

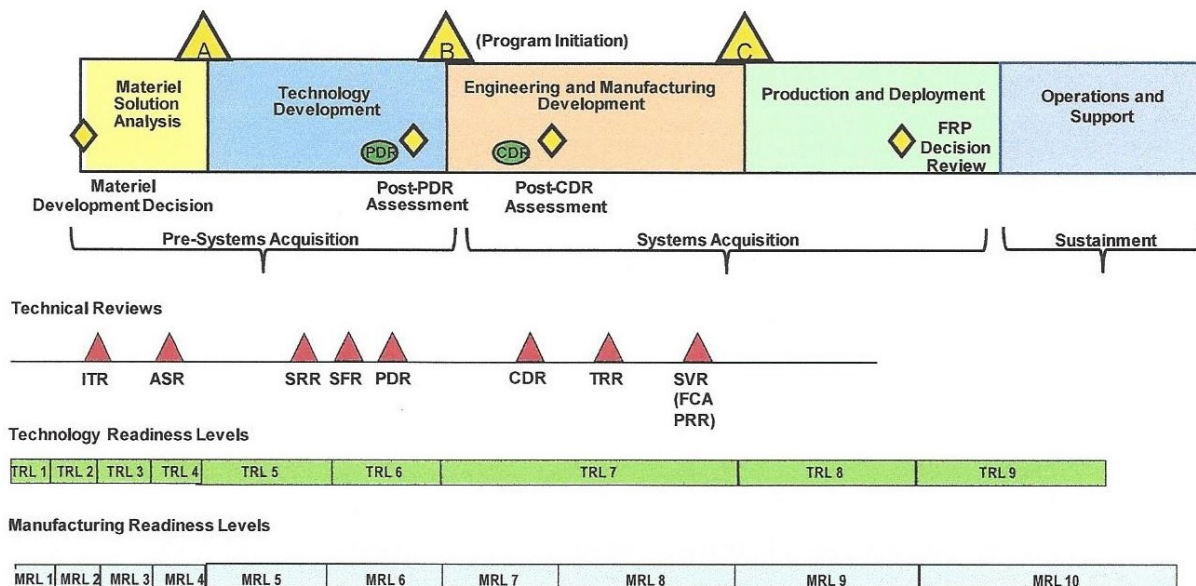


Figure 23. Relationships of MRLs to System Milestones, TRLs, and Technical Reviews [7]



NMC particles	Cathodes made of nickel manganese cobalt oxide, or NMC, are an especially hot area of battery research because they can operate at the relatively high voltages needed to store a lot of energy in a very small space. [8]
Particle size distribution, D50	The value of the particle diameter at 10%, 50% and 90% in the cumulative distribution for a group of particles expressed as D10, D50, D90, etc. Particle size distribution of D50 is also known as the median diameter or the medium value of the particle size distribution, it is the value of the particle diameter at 50% in the cumulative distribution. It is one of an important parameter characterizing particle size. For example, if D50=5.8 um, then 50% of the particles in the sample are larger than 5.8 um, and 50% smaller than 5.8 um. D50 is usually used to represent the particle size of group of particles. [9]
Pore size distribution	The distribution of the size of the various pores in a material. The range of pore sizes is divided into the groups according to IUPAC Classification of Pore Sizes: macropore >500 Angstroms, mesopore 20 to 500 Angstroms, supermicropore 7 to 20 Angstroms, and ultramicropore ,7 Angstroms. [10]
Porosimetry	An analytical technique used to determine various quantifiable aspects of a material's porous nature, such as pore diameter, total pore volume, surface area, and bulk and absolute densities [11]
Pouch cell	Instead of a metallic cylinder and glass-to-metal electrical feed-through, conductive foil-tabs are welded to the electrodes and brought to the outside in a fully sealed way with the end product resembling a pouch. [12]
Proton exchange membrane fuel cell	Type of fuel cell being developed for transport applications as well as for stationary and portable fuel cell applications [13]
Roll-to-roll	Any process of applying coatings, printing, or performing other processes starting with a roll of a flexible material and re-reeling after the process to create an output roll [14]
Slot coating die	A slot coating die is a device that is capable of holding a fluid's temperature, distributing a fluid uniformly and defining a coating width. The die is comprised of steel body sections that house the fluid flow chamber. A dual slot coating die would use an upper and lower section. [15]
Tap Density	The apparent powder density of a powder bed formed in a container of stated dimensions when a stated amount of the powder is vibrated or tapped under stated conditions [16]
Technology Readiness Level	Technology Readiness Levels (TRLs) were developed by the National Aeronautics and Space Administration (NASA) as a systematic metric/measurement system that supports assessments of the maturity of a particular technology and the consistent comparison of maturity between different types of technology as defined in Table XI. Figure 23 above provides a schematic of the relationships. [17, 18]

Table XI. Technology Readiness Level Definitions [18]

### Technology Readiness Levels

Relative Level of Technology Development	Technology Readiness Level	TRL Definition	Description
System Operations	TRL 9	Actual system operated over the full range of expected conditions.	Actual operation of the technology in its final form, under the full range of operating conditions. Examples include using the actual system with the full range of real wastes.
System Commissioning	TRL 8	Actual system completed and qualified through test and demonstration.	Technology has been proven to work in its final form and under expected conditions. In almost all cases, this TRL represents the end of true system development. Examples include developmental testing and evaluation of the system with real waste in hot commissioning.
	TRL 7	Full-scale, similar (prototypical) system demonstrated in a relevant environment	Prototype <sup>a</sup> full scale system. Represents a major step up from TRL 6, requiring demonstration of a system prototype in a relevant environment. Examples include testing the prototype in the field with a range of simulants and/or real waste and cold commissioning.
Technology Demonstration	TRL 6	Engineering scale, similar (prototypical) system validation in a relevant environment	Representative engineering scale system, which is well beyond the scale tested for TRL 5, is tested in a relevant environment. Represents a major step up in a technology's demonstrated readiness and system integration. Examples include testing a prototype with real waste and a range of simulants.
Technology Development	TRL 5	Laboratory/bench scale, similar system validation in relevant environment	The basic technological components are integrated so that the system configuration is similar to (matches) the final application in almost all respects. Examples include testing a high-fidelity system in a simulated environment and/or with a range of real wastes and simulants.
	TRL 4	Component and/or system validation in laboratory environment	Basic technological components are integrated to establish that the pieces will work together. This is relatively "low fidelity" compared with the eventual system. Examples include integration of "ad hoc" hardware in a laboratory and testing with a range of simulants. <sup>b</sup> Laboratory/bench scale testing may not be appropriate for all systems. For example, mechanical systems, such as robotic retrieval technologies, may require full scale prototype testing to meet TRL 4.
Research to Prove Feasibility	TRL 3	Analytical and experimental critical function and/or characteristic proof of concept	Active research and development is initiated. This includes analytical studies and laboratory/bench scale studies to physically validate the analytical predictions of separate elements of the technology. Examples include components that are not yet integrated or representative. Components may be tested with simulants. For some applications, such as mechanical systems, this may include computer and/or physical modeling to demonstrate functionality.
	TRL 2	Technology concept and/or application formulated	Invention begins. Once basic principles are observed, practical applications can be invented. Applications are speculative, and there may be no proof or detailed analysis to support the assumptions. Examples are still limited to analytic studies.
Basic Technology Research	TRL 1	Basic principles observed and reported	Lowest level of technology readiness. Scientific research begins to be translated into applied research and development (R&D). Examples might include paper studies of a technology's basic properties.

<sup>a</sup> A prototype is defined as a physical or virtual model used to evaluate the technical or manufacturing feasibility or utility of a particular technology or process, concept, end item, or system.

<sup>b</sup> If feasible, it is recommended to include tests on a limited range of real waste prior to achieving TRL 4.

Time-of-flight secondary ion mass spectrometry

An analytical technique that provides detailed elemental and molecular ion information about the surface, thin layers, interfaces of the sample, and gives a full three-dimensional analysis. [19]

## Webline

During the sheet printing process, after each sheet has been printed, the press table needs to be hand-wiped to ensure the ink will not smear and ruin the printed circuit. In webline printing, the machine has a wiper mechanism, automating the process. Using webline printing increases production speeds and creates a more streamlined printing process. [20]

## References

1. “Materials Genome Initiative for Global Competitiveness,” National Science and Technology Council, Executive Office of the President, Washington, DC, June 24, 2011, accessed on March 23, 2016: <http://www.whitehouse.gov/mgi>.
2. The Battery University, BU-402: What Is C-rate.  
[http://www.batteryuniversity.com/learn/article/what\\_is\\_the\\_c\\_rate](http://www.batteryuniversity.com/learn/article/what_is_the_c_rate)
3. Wikipedia. [www.en.wikipedia.org/wiki/BET\\_theory](http://www.en.wikipedia.org/wiki/BET_theory)
4. Wikipedia. [www.en.wikipedia.org/wiki/Calendering](http://www.en.wikipedia.org/wiki/Calendering)
5. The Free Dictionary. [www.encyclopedia2.thefreedictionary.com/Coin+cell](http://www.encyclopedia2.thefreedictionary.com/Coin+cell)
6. FreedomCAR Battery Test Manual For Power-Assist Hybrid Electric Vehicles, U.S. Department of Energy, Energy Efficiency and Renewable Energy, Idaho Operations Office, October 2003.  
[https://avt.inl.gov/sites/default/files/pdf/battery/freedomcar\\_manual\\_04\\_15\\_03.pdf](https://avt.inl.gov/sites/default/files/pdf/battery/freedomcar_manual_04_15_03.pdf)
7. Manufacturing Readiness Level (MRL) Deskbook Version 2.0, Prepared by the OSD Manufacturing Technology Program in collaboration with The Joint Service/Industry MRL Working Group, May, 201.
8. “A Simple Way to Make Lithium ion Battery Electrodes that Protect Themselves” SLAC Press Release on January 11, 2016. <https://www6.slac.stanford.edu/news/2016-01-11-simple-way-make-lithium-ion-battery-electrodes-protect-themselves.aspx>
9. HMKTest® website. [www.aimsizer.com/faqs-What-is-D50.html](http://www.aimsizer.com/faqs-What-is-D50.html)
10. Lastoskie, C; Keith E. Gubbins, K.E.; Quirk, N. “Pore Size Distribution Analysis of Microporous Carbons: A Density Functional Theory Approach.” J. Phys. Chem. 1993, [97], pp 4786-4796, December 4, 1992.
11. Definitions and Translations. <http://www.definitions.net/definition/porosimetry>
12. The Battery University, BU-301a: Types of Battery Cells.  
[http://www.batteryuniversity.com/learn/article/types\\_of\\_battery\\_cells](http://www.batteryuniversity.com/learn/article/types_of_battery_cells)
13. Wikipedia. [https://en.wikipedia.org/wiki/Proton\\_exchange\\_membrane\\_fuel\\_cell](https://en.wikipedia.org/wiki/Proton_exchange_membrane_fuel_cell)
14. Wikipedia. [https://en.wikipedia.org/wiki/Roll-to-roll\\_processing](https://en.wikipedia.org/wiki/Roll-to-roll_processing)
15. Miller, M.D. ‘Slot Die Coating Technology’ Extrusion Dies Industries, LLC, Chippewa Falls, WI.  
<https://www.pstc.org/files/public/Miller09.pdf>
16. Bulk Density and Tapped Density of Powders, Stage 6 Harmonization, December 1, 2012.  
[http://www.usp.org/sites/default/files/usp\\_pdf/EN/USPNF/revisions/m99375-bulk\\_density\\_and\\_tapped\\_density\\_of\\_powders.pdf](http://www.usp.org/sites/default/files/usp_pdf/EN/USPNF/revisions/m99375-bulk_density_and_tapped_density_of_powders.pdf)
17. Mankins, J. C. (April 6, 1995). Technology Readiness Levels: A White Paper, Advanced Concepts Office, Office of Space Access and Technology, National Aeronautics and Space Administration.
18. U.S. Department of Energy, Office of Environmental Management, Technology Readiness Assessment (TRA) / Technology Maturation Plan (TMP) Process Guide, March 2008
19. IONTOF Website: <https://www.iontof.com/tof-sims-secondary-ion-mass-spectrometry.html>
20. GM Nameplate website:  
<https://www.gmnameplate.com/company/blog/printing-sheet-vs-webline-printing>

## Bibliography

Risk Management. (2015). SAP-OCE&PMS-413.3B-B-05. Washington, DC 20585: U.S. Department of Energy. Access: [https://www.emcbc.doe.gov/pmsso/supporting\\_files/Risk%20Mgt.pdf](https://www.emcbc.doe.gov/pmsso/supporting_files/Risk%20Mgt.pdf)